Autism Research

WILEY | INSAR International Society for Autism Research

RESEARCH ARTICLE

Auditory P100m and Language Difficulties in Children With ASD: Effects of Vowel-Like Acoustic Structure

Kirill A. Fadeev[1] | Ilacai V. Romero Reyes[1] | Dzerassa E. Goiaeva[1] | Tatiana M. Ovsiannikova[1] | Andrey O. Prokofyev[1] | Anna M. Rytikova[1] | Artem Y. Novikov[2] | Tatiana A. Stroganova[1] | Elena V. Orekhova[1]

[1]Center for Neurocognitive Research (MEG Center), Moscow State University of Psychology and Education, Moscow, Russian Federation | [2]RNSO "Center for Curative Pedagogics", Moscow, Russian Federation

Correspondence: Elena V. Orekhova (orekhova.elena.v@gmail.com)

Received: 21 May 2025 | **Revised:** 7 February 2026 | **Accepted:** 9 March 2026

Keywords: auditory evoked fields | autism spectrum disorders (ASD) | language | magnetoencephalography (MEG) | P100m/M50/P100/ | sustained negativity

ABSTRACT

The P100/P100m component of auditory event-related potentials/fields is considered a potential biomarker of atypical arousal and language difficulties in children with ASD. When elicited by complex speech-like sounds with regular temporal or frequency structure, P100/P100m may be influenced by sustained negativity (SN), which can reduce its amplitude due to opposing current polarity and contribute to ASD-related differences. Using magnetoencephalography (MEG), we examined P100m responses to acoustic regularities in the left and right auditory cortices in 35 ASD and 39 TD boys (7–12 years). Stimuli included (1) temporally and spectrally regular sounds (periodic vowels), (2) temporally regular sounds (periodic non-vowels), (3) spectrally regular sounds (non-periodic vowels), as well as (4) non-regular control stimuli (non-periodic, non-vowels). P100m was estimated using distributed source localization. Both groups showed decreased P100m amplitude and latency with acoustic regularities, accompanied by proportional SN increases, suggesting P100m modulation primarily reflects early SN enhancement. No group differences were observed in P100m latency or amplitude, and their modulation by stimulus type was also normal in ASD, indicating spared processing of acoustic regularities in the P100m time range. However, P100m latencies variability was increased in boys with ASD, and their left P100m amplitudes to both non-regular and regular sounds were negatively associated with cumulative language and intellectual abilities. These findings suggest that while most children with ASD show typical P100m responses, individual variations in P100m amplitude may reflect neurodevelopmental differences in cortical maturation and/or sensory habituation processes that contribute to the heterogeneity of cognitive and language abilities in ASD.

1 | Introduction

Advances in understanding the neurobiology of neurodevelopmental disorders, coupled with progress in developing corresponding animal models, have highlighted the need for accessible neural biomarkers that are translatable between humans and animals. In this context, transient components of the auditory cortical evoked response are of particular interest, as they can be reliably recorded in both animal models and human populations—including those with severe impairments, such as children with fragile X syndrome (FRAX) (An et al. 2022) or Rett syndrome (Kostanian et al. 2023; see Sysoeva et al. 2020 for a review).

The maturation of the auditory cortex is associated with marked changes in the morphology of transient auditory evoked responses recorded by magnetoencephalography (MEG) and electroencephalography (EEG). Unlike adults, who exhibit a P50-N100-P200 waveform in auditory ERPs at vertex recording sites, young children typically display a

Summary

Previous studies have linked the child auditory response to language abilities in ASD. In the present study, we examined how vowel-like temporal and spectral regularities influence P100m and its association with language skills. Although group-level P100m measures were within the typical range in children with ASD, higher P100m amplitude was associated with lower language scores and IQ, irrespective of the vowel-like features of the stimuli. Given that P100m amplitude typically decreases with age and stimulus repetition, variability in its magnitude may reflect differences in the maturation of the auditory cortex or in habituation processes that are relevant for language and cognitive development in ASD.

P100-N200 complex (Ponton et al. 2000, 2002). Both the latency and amplitude of the P100 component decrease with age between approximately 6 and 12+ years (Sharma et al. 1997; Ponton et al. 2000), likely reflecting the developmental emergence of the N100 component associated with maturation of supragranular cortical layers II and III (Eggermont and Moore 2011). Some authors interpret the vertex-positive pediatric component peaking around 100 ms as an immature P50 (or M50 in MEG). However, EEG and MEG recordings from 7 to 10-year-old children have shown that an earlier, lower-amplitude P50/M50 (~65 ms) can be distinguished from a later response (~100 ms) of the same polarity under specific stimulation conditions (Stroganova et al. 2013; Orekhova et al. 2013). Furthermore, intracranial recordings in 3–7-year-old children have demonstrated a positive component at 35–60 ms, indicating that this early response is already established by age three (Korzyukov et al. 2009). Collectively, these findings challenge the interpretation of the "child" P100/P100m as merely an immature form of the adult P50/P50m. Therefore, in the present text, we employ a neutral, latency-based terminology: the large, positive, monophasic component that dominates children's EEG/MEG responses and peaks after 50 ms is designated as the P100/P100m. When citing pediatric studies that labeled this same component as P50 or P1, we retain our term (P100m), noting the original label (e.g., P50) in parentheses for clarity.

The P100/P100m is a pre-attentive component that can be reliably detected in most children. Its developmental changes reflect the maturation of the auditory cortex (Eggermont and Ponton 2003; Eggermont and Moore 2011), making it a useful marker for assessing auditory cortex plasticity in cochlear implant users implanted at various ages (Sharma et al. 2015). Multiple studies have also evaluated the characteristics of this component in children with developmental disorders characterized by atypical auditory sensory processing, such as autism spectrum disorder (ASD) (Cotter et al. 2023; Donkers et al. 2015; Haesen et al. 2011), Rett syndrome (Kostanian et al. 2023; Brima et al. 2024), or FRAX (An et al. 2022). Some research has identified relationships between P100m characteristics and children's language abilities (Yoshimura et al. 2021; Matsuzaki et al. 2020; Kautto et al. 2024; An et al. 2022; Roberts et al. 2019), suggesting that P100m (M50) latency could serve as a biomarker for language abnormalities in ASD and possibly other developmental disorders (Roberts et al. 2019, 2021). Thus, the P100m may reflect not only the structural maturation of the auditory cortex but also its functional efficiency in speech processing.

The P100m and other transient auditory response components may overlap with the sustained negativity (SN), a vertex-negative potential that persists throughout stimulus presentation when using low high-pass filters or DC recording (Picton et al. 1978). Despite developmental differences in transient components, the SN can be recorded in both children and adults (Stroganova et al. 2020; Orekhova et al. 2024). The magnitude of the SN depends on the properties of the auditory stimulation, being stronger for auditory patterns such as periodic stimuli (Keceli et al. 2012, 2015; Gutschalk et al. 2002, 2004; Gutschalk and Uppenkamp 2011; Orekhova et al. 2024), or "sound figures" characterized by either a vowel formant structure (Hewson-Stoate et al. 2006; Orekhova et al. 2024; Gutschalk and Uppenkamp 2011) or non-vocal frequency regularities (Molloy et al. 2019).

The brain rapidly detects temporal or frequency regularities, leading to an increase in the SN as early as ~40 ms post-stimulus (Molloy et al. 2019; Gutschalk et al. 2004). This early onset may reflect the activation of auditory cortical neurons involved in detecting potentially relevant sound patterns (Walker et al. 2011). After its onset, the rapidly increasing SN can modulate the properties of the P100/P100m component depending on the type and degree of regularity of the auditory pattern. However, the influence of auditory patterns on transient components of the auditory response in children has not been systematically investigated. If this influence exists, inter-subject variability in P100/P100m—including differences associated with ASD—could be affected by the auditory cortex's capacity to automatically detect such patterns. Given the language deficits common in children with ASD and other developmental conditions, it would be important to explore how speech-inherent acoustic patterns, such as periodicity (pitch) or formant structure, modulate the P100 component of the auditory evoked potentials.

Previous MEG studies in children have shown that, compared to the non-periodic non-speech complex sounds, sounds characterized by periodicity (i.e., fundamental frequency, F0), formant composition, and especially their combination in computer-generated vowels, elicit an early (< 100 ms) increase in SN in auditory cortical areas—termed the 'sustained processing negativity' (SPN) (Orekhova et al. 2024; Fadeev et al. 2024). This SPN may potentially affect P100m. *The first aim* of the present study was to investigate how vowel-characteristic regularities influence the P100m component in children's auditory cortex. Our *second aim* was to examine whether P100m parameter differences between children with ASD and typically developing (TD) children are influenced by these regularities. Since previous research has associated P100m latency (Yoshimura et al. 2021; Matsuzaki et al. 2020; Roberts et al. 2019) and amplitude (Yoshimura et al. 2013; Yoshimura et al. 2024; Kautto et al. 2024; Roberts et al. 2019) with language abilities in children, our *third aim* was to explore relationship between P100m caused by sounds with and without vowel-like regularities and overall language skills in children with ASD.

TABLE 1 | Characteristics of the samples.

	Mean ± SD (range)			
	TD	**ASD**	**Student *t*-test**	***p***
Age	Mean = 9.8 ± 1.8 (7.3–13.0) *N* = 39	Mean = 10.2 ± 1.7 (6.9–12.8) *N* = 35	0.87	0.39
MPI IQ (KABC-II)	Mean = 116.2 ± 13.3 (85–138) *N* = 39	Mean = 83.1 ± 15.8 (54–128) *N* = 34	9.7	< 0.0001
SRS	Mean = 37.6 ± 20.0 (3–84) *N* = 37	Mean = 99.5 ± 27.2 (33–157) *N* = 34	11.0	< 0.0001
SCQ	Mean = 6.3 ± 3.2 (2–16) *N* = 38	Mean = 24.8 ± 6.4 (12–35) *N* = 32	15.6	< 0.0001

Note: N—number of participants for whom information is available.

2 | Method

2.1 | Participants

The characteristics of the samples are summarized in Table 1. The study included 35 boys with ASD aged 6.9–13.0 years and 39 typically developing (TD) boys matched for age. The participants were the same cohort as in a study investigating the sustained auditory MEG response (Fadeev et al. 2024). TD children were recruited via media advertisements. None of the TD participants had any known neurological or psychiatric disorders. Participants with ASD were recruited through multiple sources, including media advertisements, consulting centers, and an educational center affiliated with the Moscow State University of Psychology and Education.

The ASD diagnosis was based on the Diagnostic and Statistical Manual of Mental Disorders (5th ed.) criteria and confirmed by a child psychiatrist (author N.A.Y.) through clinical interviews with the child and parents/caregivers. In addition, parents of all children were asked to complete the Russian translation of parental questionnaires: Social Responsiveness Scale for children (Constantino 2013) and Social Communication Questionnaire (SCQ-Lifetime; Berument et al. 1999). The results of these questionnaires have shown that our samples of ASD and TD children are very well separated on autistic traits (table 1, also see Fadeev et al. 2024 for details).

Intellectual abilities were assessed using the Kaufman Assessment Battery for Children, Second Edition (KABC-II), with the Mental Processing Index (MPI) serving as an IQ equivalent (Kaufman and Kaufman 2004). The MPI excludes tasks requiring verbal reasoning, verbal concepts, or cultural knowledge, making it suitable for evaluating nonverbal cognitive abilities in both TD children and those with ASD (Drozdick et al. 2018).

The hearing status of all participants was assessed using pure-tone air conduction audiometry with an AA-02 clinical audiometer ("Biomedilen"). Auditory thresholds were tested at 500, 1000, 2000, and 4000 Hz, and the average threshold across these four frequencies was calculated separately for each ear. All participants demonstrated normal hearing (thresholds ≤ 20 dB HL) in both ears, according to standard criteria (British Society of Audiology 2018). To prevent fatigue, MEG, MRI, and psychometric evaluations were performed over the course of 3–4 visits that occurred on separate days.

The Ethics Committee of the Moscow State University of Psychology and Education approved this study. All children provided verbal assent to participate in the research, and their caregivers provided written informed consent for participation.

2.2 | Assessment of the General Level of Language Development

Language abilities were assessed using the Russian Child Language Assessment Battery (RuCLAB; Ivanova et al. 2016; Lopukhina et al. 2019), an instrument developed to evaluate expressive and receptive language in children aged 7–12 years. The RuCLAB was specifically designed to characterize individual profiles of language impairment in children with neurodevelopmental disorders (e.g., ASD or Developmental Language Disorder) and is relatively less sensitive to individual variability among typically developing children (Gomozova et al. 2021). Twelve RuCLAB subtests assessed three major language domains: vocabulary (word production and comprehension), morphosyntax (sentence production and comprehension), and discourse (text production and comprehension). Detailed descriptions of the subtests and materials are provided in Arutiunian et al. (2022) and summarized in the supporting information of Fadeev et al. (2024).

Test administration and scoring procedures followed those described in Fadeev et al. (2024). Discourse production subtests were excluded from this analysis, as most children with ASD were unable to complete them. To quantify overall language proficiency, we calculated the arithmetic mean of the scores from all remaining subtests, hereafter termed the *total language score*.

2.3 | Stimuli

The experimental paradigm used in the present study was identical to that described in Fadeev et al. (2024). We used four types of synthetic vowel-like stimuli, previously employed by Uppenkamp et al. (2006) and downloaded from "http://medi.uni-oldenburg.de/members/stefan/phonology_1/". Five strong vowels were used: /a/ (as in caw, dawn), /e/ (ate, bait), /i/ (beat, peel), /o/ (coat, wrote), and /u/ (boot, pool).

The synthetic periodic vowels consisted of damped sinusoids that were repeated with a 12 ms period, resulting in a fundamental frequency of 83.3 Hz for each vowel. The carrier frequencies for each vowel remained fixed at the four lower formant frequencies selected from the typical range of an adult male speaker. These stimuli are hereafter referred to as periodic vowels. These regular vowel stimuli were modified, as described below, to create three additional stimulus classes: non-periodic vowels, periodic non-vowels, and non-periodic non-vowels. To disrupt periodicity, the start time of each damped sinusoid was jittered within a ±6 ms window relative to its start time in the original vowel, separately for each formant. Despite resulting in degraded voice quality (a hoarse voice), these non-periodic sounds were still perceived as vowels (see Orekhova et al. 2024 for details). To disrupt formant constancy, the carrier frequency of each subsequent damped sinusoid was randomly selected from eight possible formant frequencies used to produce regular vowels, with randomization applied separately for each formant (frequency range: formant 1 = 270–1300 Hz; formant 2 = 850–2260 Hz; formant 3 = 1750–3000 Hz; formant 4 = 3300–5500 Hz). Both periodic and non-periodic sounds with disrupted formant structure were perceived as noises rather than vowels (i.e., non-vowels). The experiment included four stimulus types: (1) periodic vowels (/a/, /i/, /o/); (2) non-periodic vowels (/a/, /u/, /e/); (3) three variants of periodic non-vowels; and (4) three variants of non-periodic non-vowels. The spectral composition of these stimuli is presented in our previous paper (Orekhova et al. 2024).

Two hundred seventy stimuli from each of the four classes were presented, with three stimulus variants equally represented within each class ($N = 90$ per variant). All stimuli were presented in random order. Each stimulus lasted 812 ms, including 10 ms rise and fall times. The interstimulus intervals (ISIs) were randomly chosen from a range of 500–800 ms. A total of 1080 stimuli were presented in three 9-min sessions, with short breaks in between.

The non-periodic non-vowels were used as control stimuli. We examined how P100m characteristics change between test conditions ("periodic vowels," "non-periodic vowels," and "periodic non-vowels") and control condition ("non-periodic non-vowels") and between TD and ASD groups.

Although the stimuli were intensity-normalized, small residual differences in the rise time of our complex acoustic stimuli remained. We estimated rise time as the time point at which the RMS, calculated using a sliding 12-ms window, reached half of the maximum of the grand average across all stimuli (Table S2). On average, periodic vowels reached this half-maximum slightly earlier than the other stimulus types (~4–5 ms), whereas differences in rise time among the remaining stimulus types were absent or minimal. To ensure that the effect of acoustic regularity on P100m latency was not driven exclusively by periodic vowels, we compared all test stimuli (periodic vowels, non-periodic vowels, and periodic non-vowels) with the non-periodic non-vowel control condition (see Section 2.7.4, Statistical Analysis).

2.4 | Procedure

Children were instructed to watch a silent video (movie or cartoon) of their choice and to ignore the auditory stimuli. The stimuli were presented diotically using a Compumedics NeuroScan Stim Audio System (P/N 1105) paired with Nicolet Biomedical TIP-300 earphones. The earphones were equipped with 90 cm plastic tubes and foam earpieces. The stimulation level was calibrated to 90 dB SPL at the output of the plastic tube. The effective bandwidth of this setup is approximately 100 Hz to 4–5 kHz. Although the fundamental frequency (F0 = 83 Hz) of the periodic stimuli lies slightly below the formal lower cutoff of the system, the perception of periodicity remained intact. This is because the harmonic components responsible for encoding pitch and timbre were well within the system's operational bandwidth, thereby preserving the perceptual integrity of the sounds.

The experiment included three blocks of 360 trials each, with each block lasting approximately 9 min. Short breaks were given between blocks. When necessary, a parent/caregiver stayed with the child in the magnetically shielded room during the recording session.

2.5 | MRI Data Acquisition and Processing

Source localization was performed for all participants using individual brain models constructed from T1-weighted images. Structural T1-weighted 3D-MPRAGE images were acquired for all participants with ASD and 28 TD participants on a Siemens Magnetom Verio 3T scanner (Siemens Medical Systems, Erlangen, Germany) with the following parameters: TR 1780 ms, TE 2.78 ms, TI 900 ms, flip angle 9°, FOV 256 × 256 mm, matrix 320 × 320, 0.8 mm isotropic voxels, 224 sagittal slices. For the remaining TD participants, images were acquired on different scanners: nine subjects on a 1.5 T Philips Intera and two subjects on a 1.5 T GE Brivo MR355/MR360. Cortical reconstructions and parcellations were generated using FreeSurfer v.7.4.1 (Dale et al. 1999; Fischl et al. 1999). Inspection of the P100m source coordinates revealed no evidence that scanner type affected component localization (see Figure S1).

2.6 | MEG Data Acquisition, Preprocessing and Source Localization

MEG data were recorded using Elekta VectorView Neuromag 306-channel MEG detector array (Helsinki, Finland) with 0.1–330 Hz bandpass filters and a 1000 Hz sampling frequency.

Group differences in P100m parameters may be affected by differences in signal-to-noise ratio, which may be lower in autistic children. To control for this, we (1) monitored children's head position during MEG recording and included only those trials where

head position and motion were below specified thresholds, and (2) equalized the number of trials between groups (see below).

Bad channels were visually identified and labeled. The signal was then preprocessed using MaxFilter software (v.2.2) to reduce external noise with the temporal signal-space separation method (tSSS) and to compensate for head movements by realigning the data to a common, optimal position for each participant. This position was determined individually as the one that resulted in the smallest average head displacement across all data epochs after motion correction.

Further preprocessing was performed using MNE-Python software (v.1.7.1) (Gramfort et al. 2013) and Python (v.3.10.16). The data were filtered with a notch filter at 50 and 100 Hz and a 110 Hz low-pass filter. Periods where peak-to-peak signal amplitude exceeded thresholds of 7e−12T for magnetometers or 7e−10T/m for gradiometers, as well as flat segments where signal amplitude was below 1e−15T for magnetometers or 1e−13T/m for gradiometers were automatically excluded from further processing. To correct for cardiac and ocular artifacts, we recorded ECG, vEOG, and hEOG and applied the signal-space projection (SSP) method. We also excluded data segments where head rotation exceeded 10 degrees/s along any of the three space axes, head velocity exceeded 4 cm/s, or head position deviated by more than 10 mm from the origin position in 3D space. The data were epoched from −0.2 to 1 s relative to stimulus onset. The mean number of artifact-free epochs was initially higher in the TD participants (TD: 997 vs. ASD: 927, $p < 0.05$). To equalize these values, we randomly removed 70 epochs for each TD participant. The resulting mean number of clean epochs per condition was 231 (range 141–340) for TD children and 231 (range 131–347) for children with ASD. The epoched data were averaged separately for each of the four experimental conditions and then baseline-corrected using the mean amplitude from the −200 to 0 ms pre-stimulus interval.

To obtain the source model, the cortical surfaces reconstructed with the FreeSurfer were triangulated using dense meshes with approximately 130,000 vertices per hemisphere. The cortical mesh was then downsampled to a grid of 4098 vertices per hemisphere, corresponding to an average inter-source distance of approximately 4.9 mm on the cortical surface.

The forward solution was computed using a single-layer boundary element model (BEM) of the inner skull. Source reconstruction of the averaged event-related fields was performed using the standardized low-resolution brain electromagnetic tomography (sLORETA; Pascual-Marqui 2002), incorporating data from both gradiometers and magnetometers. Noise covariance was estimated from the time interval of −200 to 0 ms relative to stimulus onset.

2.7 | Event-Related Fields (ERF) Analysis

2.7.1 | Sensor-Level Analysis of Magnetic Field Distribution

To visualize the magnetic field distribution on the head surface, data from all subjects were transformed to a common standard head position (0, 0, and 45 mm). The root mean square (RMS) was computed from the signals of all gradiometer sensors, separately for the four stimulus types: periodic vowels, periodic non-vowels, non-periodic vowels, and non-periodic non-vowel. Grand-average field distributions corresponding to the earliest RMS peak (P100m) and the later sustained negativity (SN) were plotted for TD and ASD groups (Figure 1).

2.7.2 | Detection of P100m Component

The amplitude and latency of the P100m component were defined in source space using each subject's individual MRI-based brain model. The region of interest (ROI) was restricted to the superior surface of the temporal lobe, which includes functionally specialized auditory cortical areas A1, 52, LBelt, PBelt, MBelt, A4, and TA2 (Glasser et al. 2016). To determine the individual amplitudes and latencies of the P100m component, we undertook a two-step procedure.

First, for each subject, we calculated the grand-averaged waveform. To this end, vertex time courses within the left and right ROIs were averaged first across four experimental conditions (periodic vowels, nonperiodic vowels, periodic non-vowels, and nonperiodic non-vowels) and then across all vertices within left and right ROIs using "stc.extract_label_time_course." We used the "mean_flip" option, which accounts for the sign of the time series at vertices whose orientation differs from the dominant direction by more than 90°. The grand-average time course was subsequently low-pass filtered at 40 Hz using a fifth-order Butterworth filter. The grand-average P100m latency was identified as the peak of the maximal positivity within the 50–140 ms time window.

Second, we calculated *single-vertex waveforms* by averaging the signal across all four conditions separately for each vertex within the ROI. We then computed the correlation between each single-vertex waveform and the grand-average waveforms in the P100m time window (50–140 ms) and identified vertices where the correlation coefficient exceeded 0.8 (Pearson's r). From these vertices, we selected five sources with maximal amplitude within a ±10 ms window centered on the grand-average P100m peak latency, which were considered to represent the subject-specific P100m generators.

Inspection of individual time courses showed that this two-step procedure reduced the probability of detecting spurious sources and allowed the characterization of the P100m component in all but one control participant. In this exceptional case, the P100m was not detected in the right hemisphere.

Since the P100m definition procedure described above assumed that the P100m sources were identical across the four experimental conditions, we performed an additional analysis to test this assumption. For this purpose, each subject's data were morphed onto the FSaverage template brain. The signal within the ROI was then low-pass filtered at 40 Hz, and source orientations were adjusted to the dominant direction. The MNI coordinates of the vertex with maximal signal amplitude in the P100m time window (50–140 ms) were identified separately for each of the four experimental conditions. For each hemisphere and MNI coordinate (X, Y, and Z), we performed a mixed ANOVA with the factors Condition and Group. No significant main effects of Condition, Group, nor any significant interactions were found (all

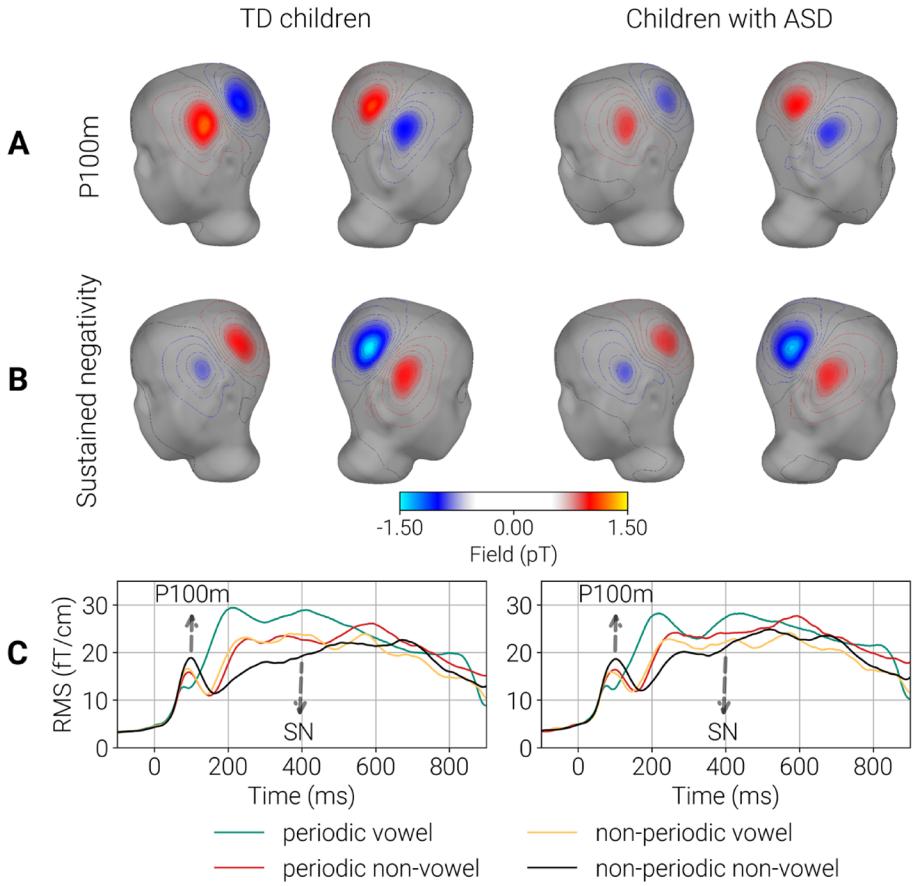

FIGURE 1 | Sensor-level auditory evoked responses. (A, B): Grand-averaged magnetic field maps for the control condition (non-periodic non-vowel), derived from gradiometer data and projected onto a standard head model. Maps are shown for the Typically Developing (TD) group (left) and the Autism Spectrum Disorder (ASD) group (right) at 100 ms (P100m; A) and 400 ms (Sustained Negativity, SN; B). The red and blue colors indicate opposite magnetic field directions (flux into the sensor plane—blue—vs. flux out of the plane—red) generated by the same dipolar cortical source. Note the reversed polarity of the P100m and SN components of the evoked magnetic field, reflecting opposite directions of the underlying cortical current flow. (C) Grand-average root mean square (RMS) waveforms across all gradiometer channels. The stimulus onset is at 0 ms; the shaded area represents the 800 ms stimulus duration. Waveforms for the test conditions (periodic vowels, non-periodic vowels, periodic non-vowels) are shown in orange, green, and red, respectively; the control condition (non-periodic non-vowel) is shown in black.

$p > 0.1$, uncorrected for multiple comparisons; see Supplementary Table S1). We therefore conclude that the assumption of common P100m sources across all conditions is valid.

2.7.3 | Estimation of Sustained Negativity (SN)

A thorough analysis of SN in children with ASD was performed by Orekhova et al. (2024). As the present study focused on the effect of the SN on the P100m component, we estimated the SN by averaging the signal from the individual P100m sources within the 200–500 ms time window—where the SN was most prominent—separately for each condition.

2.7.4 | Statistical Analysis

For statistical analysis, we used Python packages scipy (v.1.15.2), statsmodels (v.0.14.4), scikit-learn (v.1.6.1), and pingouin (v.0.5.5). We applied Levene's test to evaluate differences in variance between TD and ASD groups. To examine the between-subjects effect of Group (TD vs. ASD), and the within-subjects effects of Condition (four stimulus types) and Hemisphere on dependent variables (P100m latency and amplitude, and SF amplitude), we conducted mixed ANOVA using type III sums of squares. In this approach, each fixed factor's significance was tested after controlling for all other model factors.

We conducted repeated-measures ANOVAs with Group (ASD, TD) as a between-subjects factor and Hemisphere (left, right) and Condition (four levels) as within-subjects factors. All models included main effects and interaction terms. For any effects that violated the sphericity assumption, we applied the Greenhouse–Geisser correction and reported the adjusted degrees of freedom and p values. For P100m latency, which violated the assumption of homogeneity of variance for the between-subjects factor, we confirmed the robustness of the main effect of Group using the non-parametric Mann–Whitney U test. Post hoc comparisons between the control condition (non-periodic non-vowel) and each of the three test conditions were conducted using Wilcoxon signed-rank tests. To account for multiple comparisons, we applied a False Discovery Rate (FDR) correction using the Benjamini–Hochberg procedure to the entire set of six pairwise tests (control condition vs. three test conditions across two hemispheres).

For correlation analyses between component measures (e.g., latency and amplitude) and continuous variables (age, IQ), we used Spearman's rank correlation. Partial and semi-partial Spearman correlation coefficients were computed using the partial_corr function from the Python pingouin package. When correlation directions were consistent across all conditions (e.g., P100m amplitude–age correlations), we combined the correlation coefficients using the Fisher z-transformation method (r_{comb}). To estimate the significance of this combined statistic, we applied the Empirical Brown's Method (EBM; Poole et al. 2016), which combines dependent p values by empirically estimating the correlation structure between the tests, yielding p_{EBM}. Although EBM is designed to account for such dependencies, its accuracy in estimating the correlation matrix depends on a sufficiently large sample size. To ensure robust results with our limited sample, we complemented the EBM with a permutation test. This involved shuffling the independent variable (e.g., age and IQ) 5000 times while preserving the inherent correlation structure of the physiological variables. For each shuffle, a new combined correlation (r_{comb}) was calculated, generating a null distribution for the test statistic. Our observed statistic was then compared against this null distribution to obtain a reliable p value (p_{perm}). Both p_{EBM} and p_{perm} are reported along with the r_{comb} values.

Fisher's z-transformation was employed for the statistical comparison between correlation coefficients across groups or conditions.

3 | Results

3.1 | Sensor-Level Analysis of the Auditory ERFs

Visualization of the magnetic field distribution on the head surface model revealed that the signals at 100 ms (P100m) and 400 ms (SN) displayed opposite polarities (Figure 1, lower and upper panels). Relative to the control stimuli, stimuli characterized by temporal regularity (periodic non-vowels), formant structure (non-periodic vowels), or their combination (periodic vowels) evoked a transient reduction in the RMS amplitude around 100 ms (the P100m time window), followed by a prolonged RMS increase that persisted beyond 400 ms. The RMS amplitude reflects the average magnetic field strength independent of polarity, making it insensitive to the direction of state-dependent differences in cortical currents. Both the decreases and increases in RMS in response to vowel stimuli—compared to control non-periodic sounds lacking formant structure—reflect a sustained negative current shift in superior temporal cortex neural activity (Orekhova et al. 2024; Fadeev et al. 2024). To account for current polarity, we conducted further analysis in source space.

3.2 | Source-Level Analysis

3.2.1 | P100m Localization

The P100m component was identified in both hemispheres of all participants except one TD child, in whom it was not detected in the right hemisphere. Figure 2A shows the localization of the vertices with maximal P100m amplitude for individual subjects, while Figure 2B presents the group-level median locations. No group differences in the localization of the maximal P100m vertex were found for any MNI coordinate in either hemisphere (Mann–Whitney U test, all $p > 0.069$). In both groups, the median MNI coordinates were located within the primary auditory cortex (ASD: left hemisphere $X = -49$, $Y = -23$, $Z = 4$; right hemisphere $X = 52$, $Y = -18$, $Z = 3$. TD: left hemisphere $X = -49$, $Y = -22$, $Z = 2$; right hemisphere $X = 52$, $Y = -19$, $Z = 3$) (Figure 2B,C).

3.2.2 | P100m Latency and Amplitude in TD Children and Children With ASD

The mean P100m parameter values for TD and ASD children are presented in Table 2. The values were adjusted to the average age of 10 years using a linear model including age as a covariate. No significant group differences were found in P100m latency or amplitude for any stimulus type in either hemisphere (main effect of Group, all $p > 0.2$).

3.2.3 | Effect of Age on P100m Latency and Amplitude

Previous studies have shown that P100m latency decreases with age (Sharma et al. 2015), particularly in the right hemisphere (Roberts et al. 2019). We performed correlation analyses to determine whether this developmental decrease in P100m latency was present in our sample (Figure 3).

P100m latency decreased significantly with age in TD children (LH: $r_{comb} = -0.34$, $p_{EBM} = 0.034$, $p_{perm} = 0.017$, RH: $r_{comb} = -0.49$, $p_{EBM} < 0.0001$, $p_{perm} < 0.001$). In children with ASD, this decrease was non-significant in the left hemisphere and marginally significant in the right hemisphere (LH: $r_{comb} = -0.22$, $p_{EBM} = 0.202$, $p_{perm} = 0.16$; RH: $r_{comb} = -0.27$, $p_{ebm} = 0.05$, $p_{perm} = 0.053$). However, no significant between-group differences were found in the correlation coefficients (z-Fisher's all $p > 0.378$).

Although correlations between P100m amplitude and age were predominantly negative in both groups (ranging from $r = -0.06$ to -0.18 across hemispheres and stimulation conditions in the combined sample), none reached statistical significance (all $p > 0.13$ for the combined sample).

3.2.4 | Event-Related Time Courses of the P100m Source Activity

Comparison of the current time courses in the P100m cortical sources between the control and test stimuli revealed that periodicity, formant structure, or their combination induced a significant negative shift beginning before 100 ms and preceding the P100m peak (Figure 4). This enhanced negativity in response to the test versus control condition—termed the sustained processing negativity (SPN; Fadeev et al. 2024)—may mediate the effect of stimulus characteristics on P100m amplitude and latency. In subsequent sections, we analyze how auditory regularities (periodicity and formant composition) influence P100m latency and amplitude in children with ASD compared to TD children.

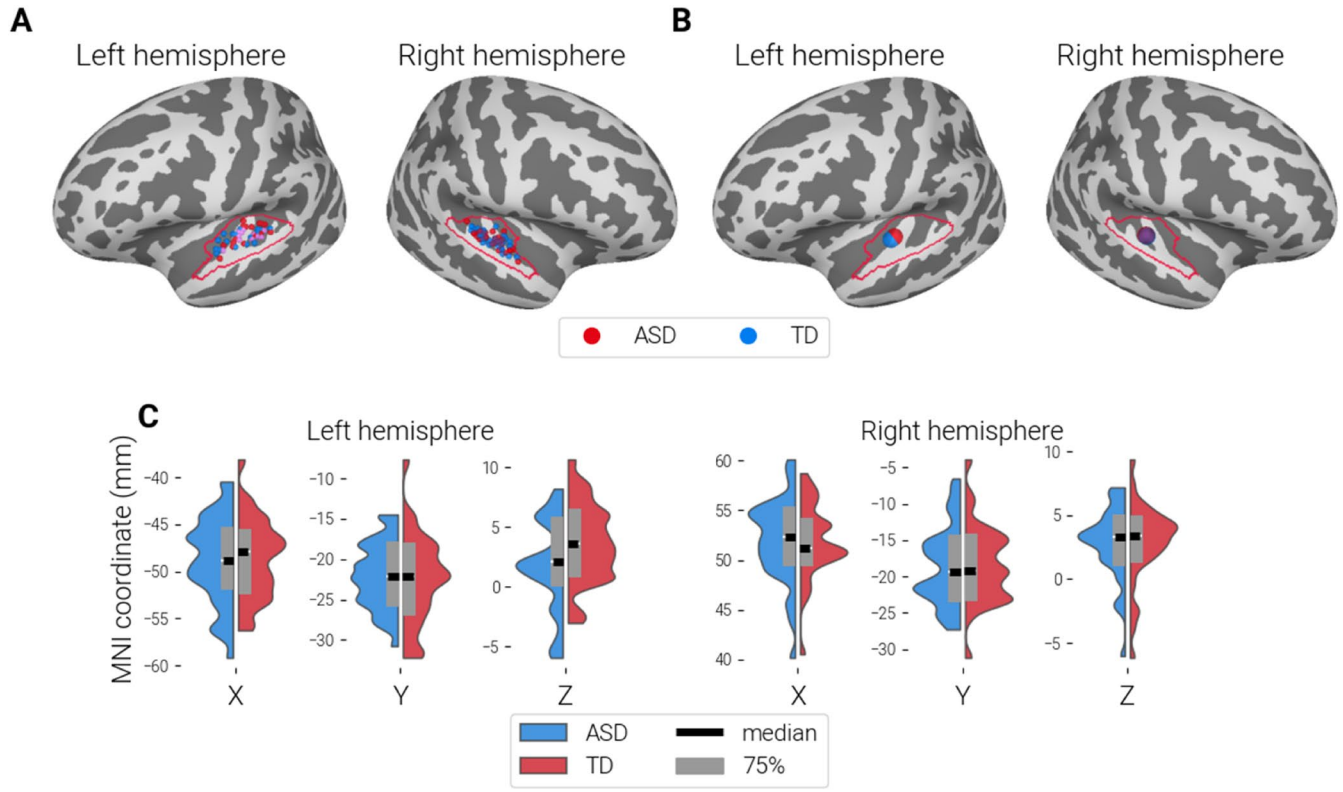

FIGURE 2 | Localization of P100m sources. (A) Individual P100m source locations ("maximal vertices") projected onto the inflated FSaverage cortical surface. Red and blue dots represent children with ASD and typically developing (TD) children, respectively. The red lines delineate the regions of interest (ROIs) used for P100m detection. (B) Group median coordinates of the P100m sources. Red and blue markers indicate the ASD and TD groups, respectively. (C) Distributions of MNI coordinates (*X*, *Y*, and *Z*) for the P100m sources in the left (LH) and right (RH) hemispheres. Violin plots show the data distribution for the TD and ASD groups, with the median and interquartile range (IQR) marked.

3.2.5 | Effects of Auditory Regularities on P100m Latency and Amplitude

For P100m latency, Levene's test indicated significantly greater variance in the ASD group compared to the TD group in the left hemisphere for periodic non-vowels ($F = 5.58$, $p = 0.021$), non-periodic vowels ($F = 5.74$, $p = 0.019$), and non-periodic non-vowels ($F = 4.76$, $p = 0.032$), and in the right hemisphere for non-periodic non-vowels ($F = 6.01$, $p = 0.016$).

ANOVA revealed a significant main effect of Condition ($F(2.01, 143.4) = 136.7$, G-G $\varepsilon = 0.67$, $p < 0.0001$, $\eta p^2 = 0.66$), which was confirmed by significant Friedman ANOVA results (left hemisphere: χ^2 ($N = 74$, $df = 3$) $= 154.6$, $p < 0.0001$; right hemisphere: χ^2 ($N = 73$, $df = 3$) $= 151.2$, $p < 0.0001$). Post hoc analysis using the Wilcoxon signed-rank test showed that P100m latency was significantly longer in the control condition versus the test conditions bilaterally (all $ps < 0.0001$; Figure 5, top panel).

A significant main effect of Hemisphere was also observed (F (1, 71) $= 31.7$, $p < 0.0001$, $\eta p^2 = 0.31$), with shorter P100m latencies in the right versus left hemisphere (Wilcoxon signed-rank test, for all conditions $p < 0.0001$). No significant main effect of Group or interactions between Group and the other factors (Condition, Hemisphere) were found for P100m latency (see Table 3).

No violation of the homogeneity of variance assumption was found for P100m amplitude (Levene's test, all $p > 0.15$). ANOVA revealed a strong main effect of Condition ($F(2.42, 171.9) = 146.9$, $p < 0.0001$, G-G $\varepsilon = 0.81$, $\eta p^2 = 0.67$). Post hoc analysis showed that P100m amplitude was significantly higher in the control condition than in the test conditions bilaterally (all $p < 0.0001$; Figure 5, bottom panel). A significant main effect of Hemisphere was also observed (F (1, 71) $= 5.10$, $p = 0.027$, $\eta p^2 = 0.07$), with higher amplitudes in the left versus right hemisphere. No significant main effect of Group or interactions involving Group were found for P100m amplitude (see Table 4).

In summary, P100m latency and amplitude demonstrated robust stimulus-dependent modulation. Consistent right-hemisphere asymmetry was observed across groups, with the right hemisphere exhibiting shorter latencies and lower amplitudes compared to the left. These patterns were equivalent in TD and ASD participants, revealing no group-specific effects.

3.2.6 | Effects of Auditory Regularities on the SN Amplitude

Evidence from Figure 4 and previous literature suggests that the increase in SN associated with regular sound processing—also known as sustained processing negativity (SPN)—emerges in the auditory cortex before the peak of the P100m component (Hewson-Stoate et al. 2006; Molloy et al. 2019; Gutschalk and Uppenkamp 2011; Fadeev et al. 2024). This enhanced SN may

TABLE 2 | P100m amplitudes and latencies in TD and ASD groups.*

	Periodic vowels		Non-periodic vowels		Periodic non-vowels		Non-periodic non-vowels	
	LH	**RH**	**LH**	**RH**	**LH**	**RH**	**LH**	**RH**
Latency P100m								
TD	82.78 ± 1.99 [78.82, 86.74]	74.13 ± 1.48 [71.18, 77.09]	93.15 ± 2.30 [88.56, 97.75]	84.43 ± 1.79 [80.85, 88.00]	94.52 ± 2.39 [89.76, 99.28]	85.75 ± 2.26 [81.25, 90.25]	98.91 ± 2.55 [93.84, 103.99]	90.06 ± 2.08 [85.92, 94.20]
ASD	81.41 ± 2.07 [77.28, 85.54]	73.34 ± 1.54 [70.26, 76.42]	92.03 ± 2.40 [87.24, 96.82]	84.88 ± 1.87 [81.15, 88.61]	97.06 ± 2.49 [92.10, 102.03]	88.02 ± 2.35 [83.32, 92.71]	99.98 ± 2.65 [94.69, 105.27]	93.17 ± 2.16 [88.85, 97.48]
Group effect (*t*-test)**	$t = 0.48$, $p = 0.636$	$t = 0.37$, $p = 0.713$	$t = 0.33$, $p = 0.739$	$t = -0.17$, $p = 0.863$	$t = -0.73$, $p = 0.466$	$t = -0.69$, $p = 0.491$	$t = -0.29$, $p = 0.773$	$t = -1.03$, $p = 0.305$
Amplitude P100m								
TD	9.67 ± 0.67 [8.35, 11.00]	7.49 ± 0.55 [6.40, 8.59]	12.50 ± 0.81 [10.89, 14.11]	10.20 ± 0.71 [8.78, 11.63]	11.93 ± 0.78 [10.39, 13.48]	9.61 ± 0.70 [8.22, 11.00]	13.53 ± 0.93 [11.68, 15.39]	11.39 ± 0.82 [9.76, 13.02]
ASD	8.88 ± 0.69 [7.50, 10.27]	8.17 ± 0.57 [7.03, 9.30]	10.99 ± 0.84 [9.31, 12.66]	10.47 ± 0.74 [8.99, 11.96]	10.87 ± 0.81 [9.26, 12.48]	10.59 ± 0.73 [9.14, 12.04]	12.86 ± 0.97 [10.93, 14.79]	12.00 ± 0.85 [10.30, 13.70]
Group effect (*t*-test)	$t = 0.82$, $p = 0.416$	$t = -0.85$, $p = 0.401$	$t = 1.29$, $p = 0.200$	$t = -0.26$, $p = 0.795$	$t = 0.94$, $p = 0.348$	$t = -0.97$, $p = 0.335$	$t = 0.50$, $p = 0.620$	$t = -0.52$, $p = 0.606$

Note: Values are presented as mean ± SE [95% CI], adjusted to the average age of 10 years.
*The data were available for all subjects ($N_{td} = 39$, $N_{asd} = 35$) in the left hemisphere and for all but one subject ($N_{td} = 38$, $N_{asd} = 35$) in the right hemisphere.
**Group differences were assessed using the *t*-statistic for the main effect of Group in the linear model; the *p* values are given without corrections for multiple comparisons.

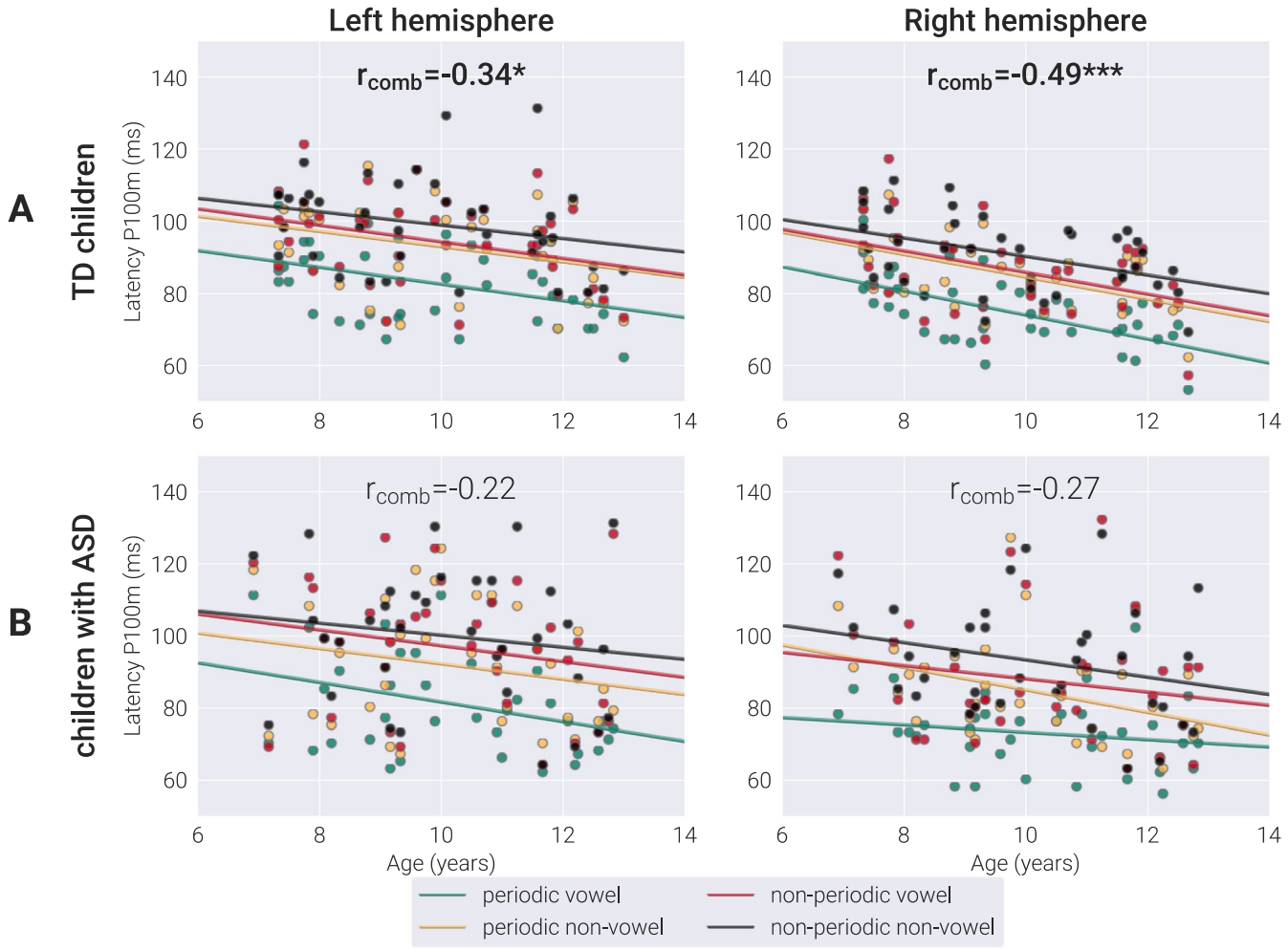

FIGURE 3 | Relationship between P100m latency and age. Scatter plots show data for (A) typically developing (TD) children and (B) children with autism spectrum disorder (ASD). Data points and regression lines are colored by experimental condition. Spearman correlation coefficients (r_{comb}) were combined across conditions using Fisher's z-transformation. *$p < 0.05$, ***$p < 0.001$. The linear regression lines are shown to illustrate age-related trends for each stimulus type; note that Spearman's correlation does not assume a linear relationship.

influence the transient P100m component of opposite polarity through spatial field spread, even if their neural sources are distinct. To assess the potential impact of the SN on the P100m, we estimated the SN from the P100m sources by averaging the signal over the 200–500 ms time window, thereby avoiding temporal overlap with the P100m component.

Previous findings have demonstrated SN enhancement by sound periodicity and/or formant composition (Gutschalk and Uppenkamp 2011; Orekhova et al. 2024). Here, we examined whether this pattern holds for the SN estimated from the P100m sources. ANOVA revealed a significant main effect of Condition on SN amplitude ($F(1.79, 127.1) = 97.1$, G-Gε = 0.60, $p < 0.0001$, $\eta p^2 = 0.58$). Post hoc analysis showed a significantly less negative SN in the control condition compared to the test conditions bilaterally (all $p < 0.0001$; Figure 6). A significant main effect of Hemisphere ($F(1, 72) = 14.5$, $p = 0.0003$, $\eta p^2 = 0.17$) reflected greater SN negativity in the right versus left hemisphere (see Table 5).

Significant main effects of Group and Group × Condition interactions were also observed (see Table 5), reflecting reduced SN responses in the ASD group compared to the TD group for stimuli containing formant structure. A significant Hemisphere × Condition interaction indicated greater right-hemispheric dominance of the SN for periodic versus non-periodic stimuli. As these effects replicate the findings of Fadeev et al. (2024) and Orekhova et al. (2024) using an alternative analytical approach, they will not be discussed further here.

Overall, the analysis of SN magnitude revealed condition-dependent differences that mirrored those observed for the P100m. Compared to the control condition, the test conditions consistently elicited a reduced positivity (P100m) and an enhanced negativity (SN) within their respective peak time windows. This effect was most pronounced for stimuli combining periodicity and formant structure. Notably, the condition eliciting the strongest P100m responses corresponded to the weakest SN magnitude, and vice versa, demonstrating an inverse relationship. A similar mirroring pattern was observed in the hemispheric asymmetry: the right hemisphere exhibited stronger negative SN currents, while the left hemisphere showed greater positive P100m currents.

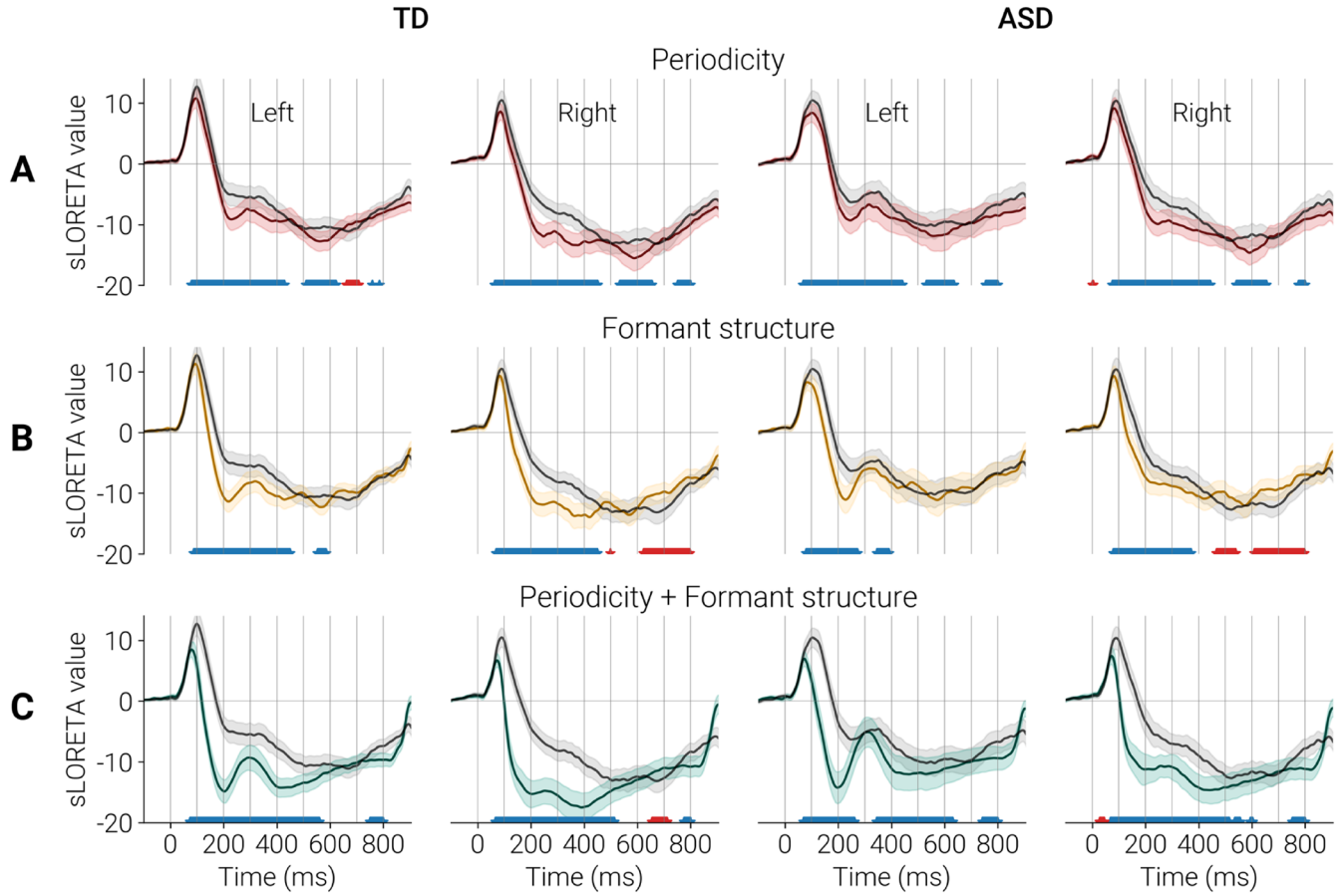

FIGURE 4 | Grand-average auditory evoked response time courses in the left and right P100m sources. Responses are shown for typically developing (TD) children and children with autism spectrum disorder (ASD). (A) The effect of periodicity (periodic non-vowel vs. control). (B) The effect of formant structure (non-periodic vowel vs. control). (C) The combined effect of periodicity and formant structure (periodic vowel vs. control). In all panels, the control condition (non-periodic non-vowel) is shown in black; test conditions are in orange (A), green (B), and red (C). Shaded areas represent the 95% confidence interval. Significant point-by-point differences between test and control conditions (paired *t*-test, $p < 0.05$, FDR-corrected) are marked below the curves: Blue asterisks indicate where the test condition is more negative than control (test < control), and red asterisks indicate where it is more positive (test > control). The sustained negative shift in response to test conditions corresponds to the sustained processing negativity (SPN).

3.2.7 | P100m Association With Language and Cognitive Abilities in ASD

Previous studies have reported associations between impaired language abilities and either delayed P100m responses (Yoshimura et al. 2013, 2021; Roberts et al. 2019) or increased P100m amplitudes (Roberts et al. 2019; Kautto et al. 2024). We examined whether general language abilities, assessed by the RuCLAB test, correlated with P100m parameters in participants with ASD. The RuCLAB test is specifically designed to evaluate language abilities in children with speech and language impairments. Consequently, TD children frequently reach a ceiling performance, precluding meaningful analysis of RuCLAB-P100m relationships in this group. For this reason, the analysis was restricted to children with ASD who had complete language and IQ scores available ($N = 31$).

Spearman partial correlation analysis (controlling for age) revealed associations between left-hemisphere P100m amplitudes and total language scores in children with ASD. While individual stimulus conditions showed varying effect sizes (periodic vowel: $r_{part} = -0.29$, $p = 0.114$; non-periodic vowel: $r_{part} = -0.43$, $p = 0.017$; periodic non-vowel: $r_{part} = -0.32$, $p = 0.083$; non-periodic non-vowel: $r_{part} = -0.42$, $p = 0.022$), the combined analysis revealed a significant negative correlation ($r_{part} = -0.37$, $p_{EBM} = 0.027$, $p_{perm} = 0.038$). This indicates that larger P100m amplitudes across stimulus conditions were associated with poorer language performance in children with ASD.

Semi-partial correlation analysis (controlling for age) similarly revealed negative associations between left-hemisphere P100m amplitudes and MPI IQ (periodic vowel: $r_{semipart} = -0.19$, $p = 0.309$; non-periodic vowel: $r_{semipart} = -0.33$, $p = 0.075$; periodic non-vowel: $r_{semipart} = -0.36$, $p = 0.049$; non-periodic non-vowel: $r_{semipart} = -0.45$, $p = 0.013$; $r_{comb} = -0.34$, $p_{EBM} = 0.043$, $p_{perm} = 0.054$).

Given the strong correlation between age-corrected language scores and MPI IQ in children with ASD ($r = 0.50$, $p = 0.005$), we performed a principal component analysis (PCA) to extract their common factor. The first principal component (PC1), termed the 'composite language and cognitive ability' factor, explained 80% of the variance and showed negative correlations with age-corrected P100m amplitudes across all stimulus conditions (periodic vowel: $r_{semipart} = -0.29$, $p = 0.115$; non-periodic vowel: $r_{semipart} = -0.48$, $p = 0.007$; periodic non-vowel: $r_{semipart} = -0.42$,

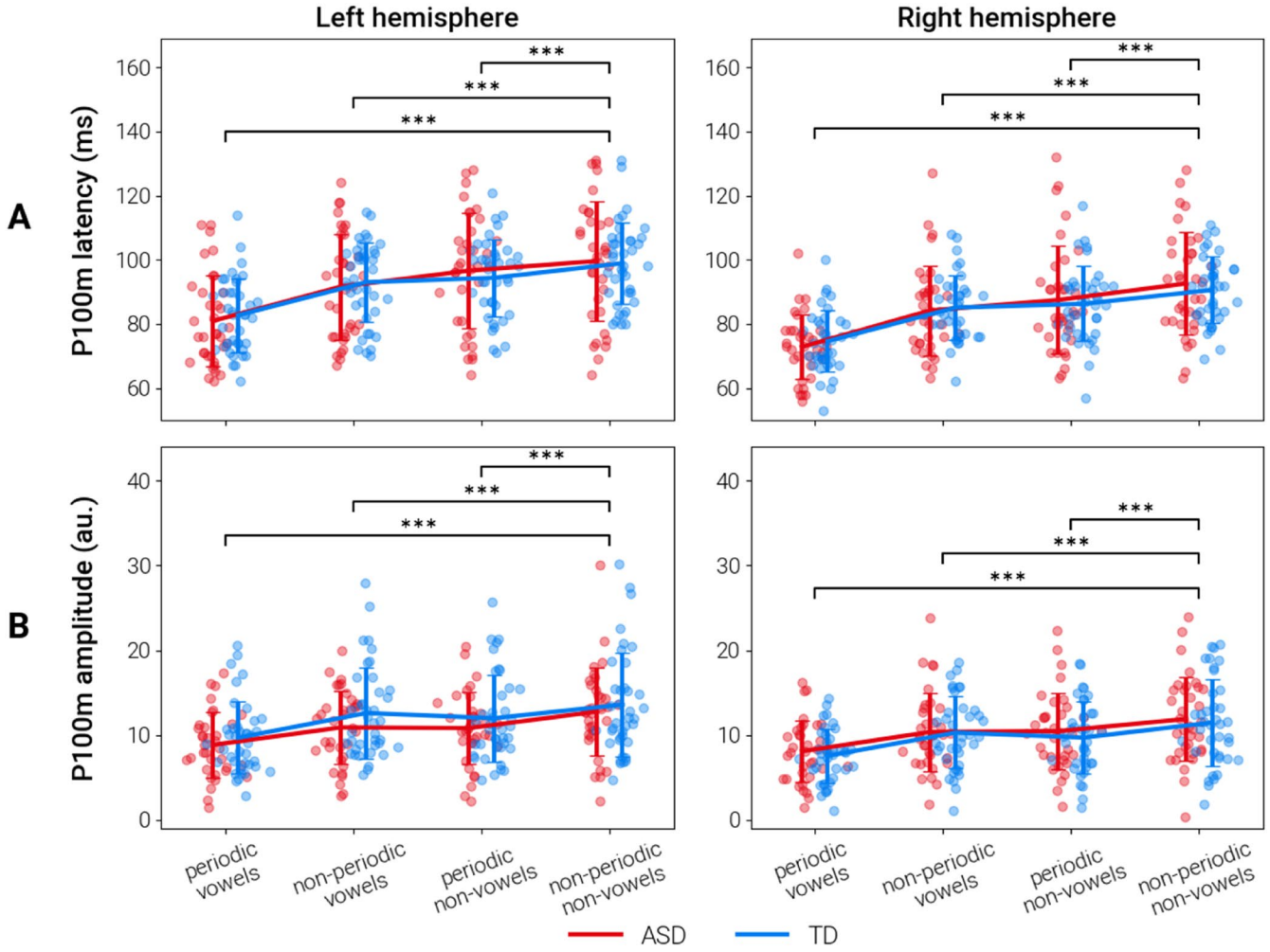

FIGURE 5 | P100m latency and amplitude in TD and ASD groups. Individual data points are shown for typically developing (TD) children and children with autism spectrum disorder (ASD). (A) P100m latency. (B) P100m amplitude. Error bars represent standard deviations. Note that statistical comparisons were performed between the control condition (non-periodic non-vowel) and each of the three test conditions. ***$p < 0.0001$ (Wilcoxon signed-rank test, FDR-corrected for the six pairwise comparisons between the control and test conditions).

TABLE 3 | Results of the mixed ANOVA for P100m latency: Effects of group, condition, and hemisphere.

Fixed factor	numDF	denDF	*F*-value	*p*	ηp^2
Group	1	71	0.01	0.925	0.00
Condition	**2.02**	**143.4**	**136.7**	**<0.0001**	**0.66**
Hemisphere	**1**	**71**	**31.7**	**<0.0001**	**0.31**
Group:Condition	2.02	143.4	1.93	0.15	0.03
Group:Hemisphere	1	71	0.06	0.81	0.00
Condition:Hemisphere	2.55	181.2	0.18	0.88	0.00
Group:Condition:Hemisphere	2.55	181.2	0.16	0.90	0.00

Note: The ANOVA was conducted with Greenhouse–Geisser correction. p = Hemisphere: $3e^{-7}$; Condition: $1e^{-15}$ (in bold).

$p = 0.022$; non-periodic non-vowel: $r_{semipart} = -0.57$, $p < 0.001$; $r_{comb} = -0.45$, $p_{EBM} = 0.005$, $p_{perm} = 0.009$; Figure 7). Notably, the presence of temporal or spectral patterns in the auditory stimuli did not significantly affect these correlations. Given the observed moderate correlation ($r_{comb} = -0.45$), our analysis with a sample size of 31 was underpowered (power = 0.68, $\alpha = 0.05$). To reliably detect an effect of this magnitude with 80% power, a future study would require a sample size of at least 39 participants.

TABLE 4 | Results of the mixed ANOVA for P100m amplitude: Effects of Group, Condition, and Hemisphere.

Fixed factor	numDF	denDF	*F* value	*p*	Partial η^2
Group	1	71	0.17	0.68	0.00
Condition	**2.42**	**171.9**	**146.9**	**<0.0001**	**0.67**
Hemisphere	**1**	**71**	**5.10**	**0.027**	**0.07**
Group:Condition	2.42	171.9	1.32	0.27	0.02
Group:Hemisphere	1	213	1.59	0.21	0.02
Condition:Hemisphere	2.33	165.1	0.11	0.92	0.00
Group:Condition:Hemisphere	2.33	165.1	0.32	0.76	0.00

Note: The ANOVA was conducted with Greenhouse–Geisser correction. p = Condition: $1e^{-15}$ (in bold).

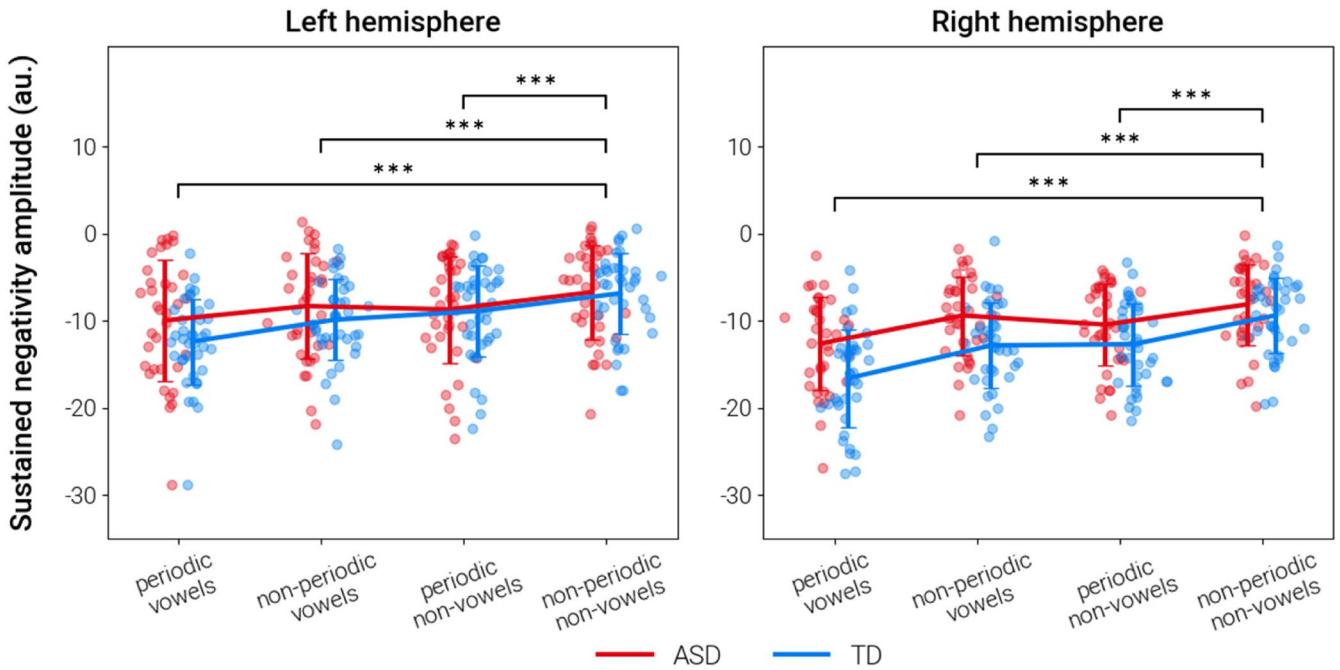

FIGURE 6 | Sustained negativity (SN) amplitude in TD and ASD groups. Individual data points are shown for typically developing (TD) children and children with autism spectrum disorder (ASD). Error bars represent standard deviations. Statistical comparisons were performed between the control condition (non-periodic non-vowel) and each of the three test conditions. ***$p < 0.0001$ (Wilcoxon signed-rank test, FDR-corrected for the six pairwise comparisons between the control and test conditions).

TABLE 5 | Results of the mixed ANOVA for sustained negativity (SN) amplitude: Effects of group, condition, and hemisphere.

Fixed factor	numDF	denDF	*F* value	*p*	Partial η^2
Group	**1**	**71**	**4.28**	**0.04**	**0.06**
Condition	**1.79**	**127.1**	**97.06**	**<0.0001**	**0.58**
Hemisphere	**1**	**71**	**14.53**	**<0.0001**	**0.17**
Group*Condition	**1.79**	**127.1**	**7.06**	**<0.0001**	**0.09**
Group*Hemisphere	1	71	1.51	0.22	0.02
Condition*Hemisphere	**2.10**	**149.1**	**5.67**	**0.001**	**0.07**
Group*Condition*Hemisphere	2.10	149.1	0.45	0.71	0.01

Note: The ANOVA was conducted with Greenhouse–Geisser correction. p = Condition: $1e^{-15}$; Hemisphere: $2.9e^{-4}$; Group*Condition: 0.002; Condition*Hemisphere: 0.004 (in bold).

While virtually no variability in language scores was observed in TD children due to a ceiling effect, they have a wide range of MPI IQ scores (85–138). Interestingly, left P100m amplitude in the TD group correlated with IQ in the direction opposite to that in the ASD group ($R = 0.34$, $p_{perm} = 0.03$, see Figure S2). This correlation, however, did not survive correction for multiple comparisons (two groups and two hemispheres).

The same correlation analysis conducted for right-hemisphere P100m amplitudes and for P100m latencies in both hemispheres revealed no significant effects (all $p > 0.22$).

4 | Discussion

This study investigated how acoustic regularities—specifically, periodicity and vowel formant structure—modulate the P100m auditory response in children, and compared these modulations between children with ASD and their TD peers. We also explored how these regularities affect the relationship between P100m characteristics and language abilities in the ASD group.

Our findings demonstrate that temporal and spectral regularities similarly reduce P100m amplitude and latency in children with ASD and their TD peers. At the group level, children with ASD showed no significant differences in P100m amplitude, latency, lateralization, or modulation. However, they exhibited greater P100m latency variability, indicating population heterogeneity and atypical auditory processing in a subset. Notably, while group-level P100m amplitudes were comparable, a stronger left-hemisphere response within the ASD group correlated with poorer language and cognitive abilities. This reveals clinically relevant neurophysiological variability that is masked in group-level analyses.

In contrast to most previous developmental studies that have used dipole fitting analysis to localize the P100m component (e.g., Roberts et al. 2010, 2013, 2019, 2020; Edgar, Fisk, et al. 2015; Edgar, Khan, et al. 2015; Green et al. 2023; Matsuzaki et al. 2020; Yoshimura et al. 2013, 2016a, 2016b, 2021; Sano et al. 2024; Parviainen et al. 2019), we implemented a distributed source localization approach. Combined with individual MRI-based brain models, this method identified the P100m component in 100% of children in the left hemisphere and in 76 of 77 children in the right hemisphere—a detection rate that meets or exceeds the rates reported in dipole source modeling studies (Roberts et al. 2010, 2020; Yoshimura et al. 2012, 2013, 2016a, 2016b, 2021; Sano et al. 2024). Our findings align with established neurodevelopmental patterns. Consistent with previous reports (Roberts et al. 2013; Sharma et al. 1997, 2015; Ponton et al. 2000), P100m latencies decreased with age (Figure 3). Furthermore, mirroring other studies (Edgar, Fisk, et al. 2015; Yoshimura et al. 2021; Green et al. 2023), latencies were shorter in the right hemisphere compared to the left (Table 2), a pattern putatively reflecting faster maturation of the right-hemispheric auditory cortex (Parviainen et al. 2019). We also replicated the left-hemisphere amplitude dominance observed in prior pediatric studies (Yoshimura et al. 2013, 2021; Sano et al. 2024; Table 2). The median MNI coordinates localized the P100m source to Heschl's gyrus in both groups, aligning with findings from intracranial recording studies (Korzyukov et al. 2009; Liégeois-Chauvel et al. 1994, 2001; see Eggermont and Ponton 2003 for review). The close alignment between our observed P100m response patterns and these established profiles supports the validity of our distributed source-based P100m detection approach.

The P100m and its EEG counterpart, the scalp-positive P1, likely reflect contributions from three central nervous system pathways: the lemniscal pathway, which projects to the primary auditory cortex (A1); the extralemniscal pathway, which terminates in secondary auditory areas that maintain dense reciprocal connections with A1; and the reticular activating system (RAS) pathway. The selective preservation of the P100m response in

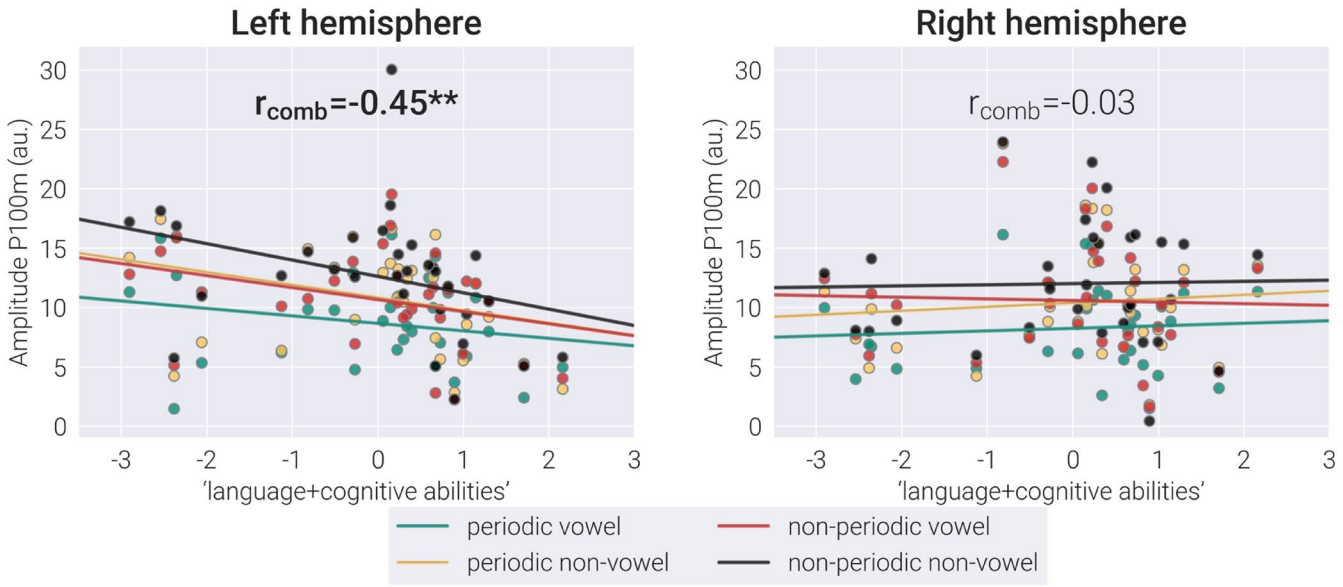

FIGURE 7 | Association between P100m amplitude and composite language/cognitive ability in children with ASD. Scatter plots show age-corrected P100m amplitudes in the left hemisphere versus the principal component analysis (PCA)-derived composite IQ-Language score. Colored lines represent the regression lines for each stimulus condition. Spearman correlation coefficients (*r*s) were combined across conditions using Fisher's z-transformation. $^{**}p < 0.01$.

children with prolonged deafness—in contrast to their absent N1 component—suggests a strong contribution from non-specific thalamocortical projections, particularly those originating in the reticular activating system, or RAS (Eggermont and Moore 2011).

Previous research has demonstrated that the P50 in adults is modulated by preattentive arousal to novel auditory stimuli (Pratt et al. 2008), and that its habituation represents a neural correlate of the brain's ability to filter out irrelevant, repetitive input (Sinclair et al. 2017). Mirroring this P50 modulation in adults, the P100/P100m in children is also influenced by arousal to temporal novelty: its amplitude increases at long interstimulus intervals and is attenuated during short-interval repetition, reflecting habituation (Orekhova et al. 2013; Stroganova et al. 2013). Based on this, one would predict that perceptually salient periodic vowels (Fadeev et al. 2024) would elicit the strongest arousal and thus the largest P100m responses. Contrary to this prediction, our findings revealed the opposite pattern: periodic vowels evoked the smallest P100m amplitudes, while unstructured control sounds produced the largest responses. Sounds containing only temporal regularity (periodic non-vowels) or only spectral regularity (non-periodic vowels) elicited intermediate amplitudes (Figure 5).

We propose that the observed inverse relationship between P100m amplitude and stimulus salience arises from temporal overlap with SPN associated with processing of temporal or spectral regularities. The SPN emerges during the P100m time window and persists for over 400 ms post-stimulus onset (figure 4; see also Orekhova et al. 2024; Fadeev et al. 2024). Critically, stimulus-related modulations of the positive-going P100m component exhibit a pattern directly opposite to that of the negative-going SN measured in the 200–500 ms interval (Figures 5 and 6).

The progressive enhancement of the SN—from control stimuli (lacking regularity) to test stimuli containing either temporal or spectral regularity, and ultimately to the 'most regular' test stimulus (periodic vowels)—likely reflects the incremental activation of neural populations specialized for detecting the auditory patterns that characterize ecologically relevant sounds such as vocalizations (Wang 2018). Wang and colleagues (Bendor and Wang 2005; Wang 2007; Wang et al. 2008) described a class of auditory neurons that respond to periodic sounds with sustained firing, which is not timed to the onset of each individual sound pulse in a periodic sequence (so-called "unsynchronized neurons"). Similarly, neurons that respond tonically to certain frequency compositions characteristic of conspecific vocalizations (Tian et al. 2001) may account for the increased SN in response to vowels devoid of periodicity. Hence, the response to periodic vowels may reflect the joint activity of these neuronal populations. Studies in humans (Molloy et al. 2019) and animals (Walker et al. 2011) show that auditory patterns are detected very rapidly and can begin modulating evoked responses as early as ~40 ms after stimulus onset—well before the P100m reaches its peak. Although our synthetic vowels had a fixed periodicity—unlike natural vowels, where the fundamental frequency (F0) typically varies over time—our findings strongly suggest that the phonetic features of natural vowels would likewise modulate P100m responses.

Taken together, our findings suggest that auditory cortex activity during the P100m time window reflects at least two distinct neural processes: (1) a phasic, surface-positive component that matures early, peaks around 100 ms post-stimulus in response to any detectable auditory input, and originates primarily from cortical layers IIIc and IV (Eggermont and Ponton 2003; Eggermont and Moore 2011); and (2) a sustained, surface-negative activity originating in supragranular layers II and III, which becomes more pronounced during the encoding of behaviorally relevant sounds containing temporal regularities or distinct spectral characteristics (Wang 2007). These processes exert opposing influences on the net P100m amplitude. Consequently, variability in the strength or timing of either process may underlie the previously reported differences in P100m parameters between children with ASD and their TD peers during speech sound processing (Yoshimura et al. 2013, 2016b; Sano et al. 2024).

Our study revealed no significant group differences in mean P100m amplitudes or latencies between children with ASD and their TD peers across all stimulus conditions. The absence of P100m amplitude differences in ASD is consistent with recent meta-analytic findings (Williams et al. 2020). However, the lack of latency differences contrasts with several previous studies reporting delayed P100m responses in ASD (Roberts et al. 2013, 2019, 2020; Matsuzaki et al. 2020; see also Williams et al. 2020). Several factors may account for this discrepancy. First, the pronounced heterogeneity within the ASD population is evident in our data, as P100m latency variance was significantly greater in the ASD group than in TD controls. Notably, for the control stimulus—which elicited the strongest P100m responses—the ASD group included both the shortest and longest latency values observed in the study (Figure 5, upper panel). Second, stimulus characteristics may play a role. While previous studies reporting P100m delays in ASD typically used pure tones, we employed spectrally complex sounds. In line with this, Yoshimura and colleagues, who also used complex auditory stimuli (e.g., the Japanese syllable /ne/), reported either typical (Yoshimura et al. 2013) or even shorter (Yoshimura et al. 2016b, 2021) P100m latencies in their ASD participants compared to TD controls.

Building on prior research demonstrating associations between P100m characteristics and language abilities (Yoshimura et al. 2013, 2021; Roberts et al. 2019; Kautto et al. 2024), we expected to observe similar relationships in our study. We focused this analysis exclusively on the ASD group because the TD children consistently performed at ceiling on the language assessment. Given the strong correlation between language and cognitive abilities within the ASD group, combined with our limited sample size, we were unable to reliably dissociate their influences. We therefore employed a composite measure of language and cognitive abilities for this analysis.

We found a significant inverse relationship between P100m amplitude and combined language-cognitive scores in the autistic participants. This finding aligns with Roberts et al. (2019), who reported larger P100m amplitudes in response to pure tones in minimally verbal children with ASD compared to their more verbal peers. The left-hemispheric specificity of this association in our ASD group supports the idea that dysfunction within left-hemispheric auditory networks may have particularly adverse effects on language development. In our study, this association

was significant for responses to non-periodic non-vowels, periodic non-vowels, and non-periodic vowels, but not for periodic vowels. The non-significant correlations for periodic vowels likely resulted from a low signal-to-noise ratio, which may have obscured the relationship. Conversely, the presence of this correlation for both control sounds and sounds with a single acoustic regularity suggests the association reflects a general neural mechanism that modulates P100m responses to diverse auditory inputs, rather than a process specific to certain sound features. This association may have at least two non-mutually exclusive explanations.

First, more severely affected children with ASD may exhibit delayed maturation of the transient N100 component, which originates from distinct auditory cortical circuitry that matures later than the P100-generating networks (Eggermont and Moore 2011). Because the N100 typically emerges in a time window partially overlapping with the P100 (Orekhova et al. 2013), its progressive maturation may attenuate the late portion of the P100m, thereby reducing its peak amplitude. Although our paradigm used short ISIs that did not elicit a distinct N100m peak (Budd et al. 1998; Čeponien et al. 1998), the underlying maturational processes may still have influenced P100m characteristics.

Second, more severely affected children with ASD may exhibit deficient habituation or sensory gating, which could manifest as elevated P100m amplitudes. This interpretation is consistent with findings of P50/P100m habituation deficits in ASD (Ruiz-Martínez et al. 2020; Orekhova et al. 2008), where the severity of the sensory impairment has been shown to correlate with the degree of intellectual disability (Orekhova et al. 2008).

Although P100m amplitude was negatively associated with psychometric scores in children with ASD, the amplitudes themselves were within the typical range (Table 2). This absence of a group-level difference may be explained by countervailing factors associated with ASD, such as increased neural noise. This noise could enhance response variability and thereby reduce the measurable P100m amplitude (Milne 2011; David et al. 2016; Raul et al. 2024).

Interestingly, in TD children, left-hemispheric P100m amplitude also tended to correlate with IQ scores; however, in this case, higher P100m amplitude was associated with higher IQ. Previous studies in TD children have likewise linked larger P100m amplitudes to better cognitive abilities (An et al. 2020; Yoshimura et al. 2014). Together, these findings suggest that the factors contributing to P100m amplitude may differ between children with ASD and those with typical development.

Our study has several limitations. First, the sample size was relatively small. Given the moderate effect size of our primary finding ($r_{comb} = -0.45$), future studies would require approximately 40 participants to achieve 80% power for replicating the observed association between P100m amplitude and language-cognitive scores in children with ASD. Furthermore, since many participants with ASD had below-average intelligence, the observed P100m effects may not be specific to ASD but could also be associated with intellectual disability. Future studies including a control group of children with below-average IQ without ASD are needed to clarify this point.

Our findings carry important methodological implications for P100/P100m research in clinical populations. When studying the transient P100/P100m component, irregular auditory stimuli (e.g., noise bursts) appear superior for reliable component identification, as they evoke robust responses with favorable signal-to-noise characteristics. Conversely, patterned stimuli such as vowels typically elicit attenuated P100/P100m amplitudes with poorer signal quality, which can compromise accurate parameter estimation.

5 | Conclusion

In summary, our findings demonstrate that P100m responses to temporally or spectrally regular sounds integrate at least two distinct neural mechanisms: (1) a phasic component reflecting sound detection and preattentive arousal, and (2) a sustained component involved in auditory pattern processing. The interplay of these processes likely underlies the variability in P100m characteristics observed across clinical populations.

Although we found no significant group-level differences in P100m amplitudes or latencies between children with ASD and their TD peers, this does not imply typical P100m generation in ASD. Notably, the ASD group exhibited substantially greater P100m latency variability than TD controls, suggesting neurobiological heterogeneity that may encompass distinct subgroups—some showing atypically prolonged latencies (consistent with Roberts et al. 2013, 2019; Matsuzaki et al. 2020) and others demonstrating atypically short latencies (consistent with Yoshimura et al. 2016b, 2021). Furthermore, in children with ASD, larger P100m amplitudes in the left hemisphere—particularly in response to non-patterned sounds—were negatively correlated with language and cognitive performance. This association may indicate an adverse impact of atypical pre-attentive auditory arousal or habituation, or of delayed auditory cortex maturation, on language and general cognitive functioning in this population.

These results underscore the complex relationship between auditory P100m responses and language impairments in ASD, a relationship that appears to arise from the interplay of multiple neural mechanisms. Further studies that delineate these underlying processes and include diverse clinical cohorts are needed to determine whether this auditory response component can serve as a clinically useful biomarker for ASD.

Acknowledgments

The study was conducted at the unique research facility "Center for Neurocognitive Research (MEG-Center)" of MSUPE.

Funding

This work was supported by the Russian Science Foundation (project # 25-18-00739).

Ethics Statement

The Ethics Committee of the Moscow State University of Psychology and Education approved this study. All children provided verbal assent to participate in the research, and their caregivers provided written informed consent for participation.

Conflicts of Interest

The authors declare no conflicts of interest.

Data Availability Statement

The de-identified individual-level raw data that supports this research, study materials, and analysis code used to generate the results are publicly available at https://openneuro.org/datasets/ds005234.

References

An, K. M., C. Hasegawa, T. Hirosawa, et al. 2020. "Brain Responses to Human-Voice Processing Predict Child Development and Intelligence." *Human Brain Mapping* 41, no. 9: 2292–2301. https://doi.org/10.1002/hbm.24946.

An, W. W., C. A. Nelson, and C. L. Wilkinson. 2022. "Neural Response to Repeated Auditory Stimuli and Its Association With Early Language Ability in Male Children With Fragile X Syndrome." *Frontiers in Integrative Neuroscience* 16: 987184. https://doi.org/10.3389/fnint.2022.987184.

Arutiunian, V., A. Lopukhina, A. Minnigulova, et al. 2022. "Language Abilities of Russian Primary-School-Aged Children With Autism Spectrum Disorder: Evidence From Comprehensive Assessment." *Journal of Autism and Developmental Disorders* 52, no. 2: 584–599. https://doi.org/10.1007/s10803-021-04967-0.

Bendor, D., and X. Wang. 2005. "The Neuronal Representation of Pitch in Primate Auditory Cortex." *Nature* 436, no. 7054: 1161–1165. https://doi.org/10.1038/nature03867.

Berument, S. K., M. Rutter, C. Lord, A. Pickles, and A. Bailey. 1999. "Autism Screening Questionnaire: Diagnostic Validity." *British Journal of Psychiatry* 175, no. 5: 444–451. https://doi.org/10.1192/bjp.175.5.444.

Brima, T., S. Beker, K. D. Prinsloo, et al. 2024. "Probing a Neural Unreliability Account of Auditory Sensory Processing Atypicalities in Rett Syndrome." *Journal of Neurodevelopmental Disorders* 16, no. 1: 28. https://doi.org/10.1186/s11689-024-09544-x.

British Society of Audiology. 2018. Recommended Procedure: Pure-Tone Air-Conduction and Bone-Conduction Threshold Audiometry With and Without Masking.

Budd, T., R. J. Barry, E. Gordon, C. Rennie, and P. Michie. 1998. "Decrement of the N1 Auditory Event-Related Potential With Stimulus Repetition: Habituation vs. Refractoriness." *International Journal of Psychophysiology* 31, no. 1: 51–68. https://doi.org/10.1016/s0167-8760(98)00040-3.

Čeponien, R., M. Cheour, and R. Näätänen. 1998. "Interstimulus Interval and Auditory Event-Related Potentials in Children: Evidence for Multiple Generators." *Electroencephalography and Clinical Neurophysiology/Evoked Potentials Section* 108, no. 4: 345–354. https://doi.org/10.1016/s0168-5597(97)00081-6.

Constantino, J. N. 2013. "Social Responsiveness Scale." In *Encyclopedia of Autism Spectrum Disorders*, 2919–2929. Springer.

Cotter, M., S. Reisli, A. A. Francisco, et al. 2023. "Neurophysiological Measures of Auditory Sensory Processing are Associated With Adaptive Behavior in Children With Autism Spectrum Disorder." *Journal of Neurodevelopmental Disorders* 15, no. 1: 11. https://doi.org/10.1186/s11689-023-09480-2.

Dale, A. M., B. Fischl, and M. I. Sereno. 1999. "Cortical Surface-Based Analysis." *NeuroImage* 9, no. 2: 179–194. https://doi.org/10.1006/nimg.1998.0395.

David, N., T. R. Schneider, I. Peiker, R. Al-Jawahiri, A. K. Engel, and E. Milne. 2016. "Variability of Cortical Oscillation Patterns: A Possible Endophenotype in Autism Spectrum Disorders?" *Neuroscience & Biobehavioral Reviews* 71: 590–600. https://doi.org/10.1016/j.neubiorev.2016.09.031.

Donkers, F. C. L., S. E. Schipul, G. T. Baranek, et al. 2015. "Attenuated Auditory Event-Related Potentials and Associations With Atypical Sensory Response Patterns in Children With Autism." *Journal of Autism and Developmental Disorders* 45, no. 2: 506–523. https://doi.org/10.1007/s10803-013-1948-y.

Drozdick, L. W., J. K. Singer, E. O. Lichtenberger, J. C. Kaufman, A. S. Kaufman, and N. L. Kaufman. 2018. "The Kaufman Assessment Battery for Children- Second Edition and KABC-II Normative Update." In *Contemporary Intellectual Assessment, Fourth Edition: Theories, Tests, and Issues*, edited by D. P. Flanagan and E. M. McDonough, 333–359. Guilford Press.

Edgar, J. C., C. L. Fisk, J. I. Iv, et al. 2015. "Auditory Encoding Abnormalities in Children With Autism Spectrum Disorder Suggest Delayed Development of Auditory Cortex." *Molecular Autism* 6, no. 1: 69. https://doi.org/10.1186/s13229-015-0065-5.

Edgar, J. C., S. Y. Khan, L. Blaskey, et al. 2015. "Neuromagnetic Oscillations Predict Evoked-Response Latency Delays and Core Language Deficits in Autism Spectrum Disorders." *Journal of Autism and Developmental Disorders* 45, no. 2: 395–405. https://doi.org/10.1007/s10803-013-1904-x.

Eggermont, J. J., and J. K. Moore. 2011. "Morphological and Functional Development of the Auditory Nervous System." In *Springer Handbook of Auditory Research*, 61–105. Springer. https://doi.org/10.1007/978-1-4614-1421-6_3.

Eggermont, J. J., and C. W. Ponton. 2003. "Auditory-Evoked Potential Studies of Cortical Maturation in Normal Hearing and Implanted Children: Correlations With Changes in Structure and Speech Perception." *Acta Oto-Laryngologica* 123, no. 2: 249–252. https://doi.org/10.1080/0036554021000028098.

Fadeev, K. A., I. V. Romero Reyes, D. E. Goiaeva, et al. 2024. "Attenuated Processing of Vowels in the Left Temporal Cortex Predicts Speech-In-Noise Perception Deficit in Children With Autism." *Journal of Neurodevelopmental Disorders* 16, no. 1: 67. https://doi.org/10.1186/s11689-024-09585-2.

Fischl, B., M. I. Sereno, and A. M. Dale. 1999. "Cortical Surface-Based Analysis." *NeuroImage* 9, no. 2: 195–207. https://doi.org/10.1006/nimg.1998.0396.

Glasser, M. F., T. S. Coalson, E. C. Robinson, et al. 2016. "A Multi-Modal Parcellation of Human Cerebral Cortex." *Nature* 536, no. 7615: 171–178. https://doi.org/10.1038/nature18933.

Gomozova, M., V. Arutiunian, A. Lopukhina, and O. Dragoy. 2021. "Russian Child Language Assessment Battery (RuCLAB) and Its Application in Primary School Children With ASD." *Autism and Developmental Disorders* 19, no. 4: 24–31. https://doi.org/10.17759/autdd.2021190403.

Gramfort, A., M. Luessi, E. Larson, et al. 2013. "MEG and EEG Data Analysis With MNE-Python." *Frontiers in Neuroscience* 7: 267. https://doi.org/10.3389/fnins.2013.00267.

Green, H. L., G. Shen, R. E. Franzen, et al. 2023. "Differential Maturation of Auditory Cortex Activity in Young Children With Autism and Typical Development." *Journal of Autism and Developmental Disorders* 53, no. 10: 4076–4089. https://doi.org/10.1007/s10803-022-05696-8.

Gutschalk, A., R. D. Patterson, A. Rupp, S. Uppenkamp, and M. Scherg. 2002. "Sustained Magnetic Fields Reveal Separate Sites for Sound Level and Temporal Regularity in Human Auditory Cortex." *NeuroImage* 15, no. 1: 207–216. https://doi.org/10.1006/nimg.2001.0949.

Gutschalk, A., R. D. Patterson, M. Scherg, S. Uppenkamp, and A. Rupp. 2004. "Temporal Dynamics of Pitch in Human Auditory Cortex." *NeuroImage* 22, no. 2: 755–766. https://doi.org/10.1016/j.neuroimage.2004.01.025.

Gutschalk, A., and S. Uppenkamp. 2011. "Sustained Responses for Pitch and Vowels Map to Similar Sites in Human Auditory Cortex."

NeuroImage 56, no. 3: 1578–1587. https://doi.org/10.1016/j.neuroimage.2011.02.026.

Haesen, B., B. Boets, and J. Wagemans. 2011. "A Review of Behavioural and Electrophysiological Studies on Auditory Processing and Speech Perception in Autism Spectrum Disorders." *Research in Autism Spectrum Disorders* 5, no. 2: 701–714. https://doi.org/10.1016/j.rasd.2010.11.006.

Hewson-Stoate, N., M. Schönwiesner, and K. Krumbholz. 2006. "Vowel Processing Evokes a Large Sustained Response Anterior to Primary Auditory Cortex." *European Journal of Neuroscience* 24, no. 9: 2661–2671. https://doi.org/10.1111/j.1460-9568.2006.05096.x.

Ivanova, I., D. Dragoy, A. Akinina, et al. 2016. "AutoRAT at Your Fingertips: Introducing the New Russian Aphasia Test on a Tablet." *Frontiers in Psychology* 7. https://doi.org/10.3389/conf.fpsyg.2016.68.00116.

Kaufman, A. S., and N. L. Kaufman. 2004. *Kaufman Test of Educational Achievement*. 2nd ed. American Guidance Service.

Kautto, A., H. Railo, and E. Mainela-Arnold. 2024. "Low-Level Auditory Processing Correlates With Language Abilities: An ERP Study Investigating Sequence Learning and Auditory Processing in School-Aged Children." *Neurobiology of Language* 5, no. 2: 341–359. https://doi.org/10.1162/nol_a_00129.

Keceli, S., K. Inui, H. Okamoto, N. Otsuru, and R. Kakigi. 2012. "Auditory Sustained Field Responses to Periodic Noise." *BMC Neuroscience* 13, no. 1: 7. https://doi.org/10.1186/1471-2202-13-7.

Keceli, S., H. Okamoto, and R. Kakigi. 2015. "Hierarchical Neural Encoding of Temporal Regularity in the Human Auditory Cortex." *Brain Topography* 28, no. 3: 459–470. https://doi.org/10.1007/s10548-013-0300-3.

Korzyukov, O., E. Asano, V. Gumenyuk, et al. 2009. "Intracranial Recording and Source Localization of Auditory Brain Responses Elicited at the 50 Ms Latency in Three Children Aged From 3 to 16 Years." *Brain Topography* 22, no. 3: 166–175. https://doi.org/10.1007/s10548-009-0108-3.

Kostanian, D., A. Rebreikina, V. Voinova, and O. Sysoeva. 2023. "Effect of Presentation Rate on Auditory Processing in Rett Syndrome: Event-Related Potential Study." *Molecular Autism* 14, no. 1: 40. https://doi.org/10.1186/s13229-023-00566-1.

Liégeois-chauvel, C., K. Giraud, J. Badier, P. Marquis, and P. Chauvel. 2001. "Intracerebral Evoked Potentials in Pitch Perception Reveal a Functional Asymmetry of the Human Auditory Cortex." *Annals of the New York Academy of Sciences* 930, no. 1: 117–132. https://doi.org/10.1111/j.1749-6632.2001.tb05728.x.

Liégeois-Chauvel, C., A. Musolino, J. Badier, P. Marquis, and P. Chauvel. 1994. "Evoked Potentials Recorded From the Auditory Cortex in Man: Evaluation and Topography of the Middle Latency Components." *Electroencephalography and Clinical Neurophysiology/Evoked Potentials Section* 92, no. 3: 204–214. https://doi.org/10.1016/0168-5597(94)90064-7.

Lopukhina, A., A. Chrabaszcz, M. Khudyakova, I. Korkina, A. Yurchenko, and O. Dragoy. 2019. Test for Assessment of Language Development in Russian «KORABLIK». In Proceedings of the Satellite of AMLaP Conference (Typical and Atypical Language Development Symposium).

Matsuzaki, J., M. Ku, M. Dipiero, et al. 2020. "Delayed Auditory Evoked Responses in Autism Spectrum Disorder Across the Life Span." *Developmental Neuroscience* 41, no. 3–4: 223–233. https://doi.org/10.1159/000504960.

Milne, E. 2011. "Increased Intra-Participant Variability in Children With Autistic Spectrum Disorders: Evidence From Single-Trial Analysis of Evoked EEG." *Frontiers in Psychology* 2: 51. https://doi.org/10.3389/fpsyg.2011.00051.

Molloy, K., N. Lavie, and M. Chait. 2019. "Auditory Figure-Ground Segregation Is Impaired by High Visual Load." *Journal of Neuroscience* 39, no. 9: 1699–1708. https://doi.org/10.1523/jneurosci.2518-18.2018.

Orekhova, E. V., A. V. Butorina, M. M. Tsetlin, et al. 2013. "Auditory Magnetic Response to Clicks in Children and Adults: Its Components, Hemispheric Lateralization and Repetition Suppression Effect." *Brain Topography* 26, no. 3: 410–427. https://doi.org/10.1007/s10548-012-0262-x.

Orekhova, E. V., K. A. Fadeev, D. E. Goiaeva, et al. 2024. "Different Hemispheric Lateralization for Periodicity and Formant Structure of Vowels in the Auditory Cortex and Its Changes Between Childhood and Adulthood." *Cortex* 171: 287–307. https://doi.org/10.1016/j.cortex.2023.10.020.

Orekhova, E. V., T. A. Stroganova, A. O. Prokofyev, G. Nygren, C. Gillberg, and M. Elam. 2008. "Sensory Gating in Young Children With Autism: Relation to Age, IQ, and EEG Gamma Oscillations." *Neuroscience Letters* 434, no. 2: 218–223. https://doi.org/10.1016/j.neulet.2008.01.066.

Parviainen, T., P. Helenius, and R. Salmelin. 2019. "Children Show Hemispheric Differences in the Basic Auditory Response Properties." *Human Brain Mapping* 40, no. 9: 2699–2710. https://doi.org/10.1002/hbm.24553.

Pascual-Marqui, R. D. 2002. "Standardized Low-Resolution Brain Electromagnetic Tomography (sLORETA): Technical Details." *PubMed* 24 Suppl D: 5–12. https://pubmed.ncbi.nlm.nih.gov/12575463.

Picton, T., D. Woods, and G. Proulx. 1978. "Human Auditory Sustained Potentials. II. Stimulus Relationships." *Electroencephalography and Clinical Neurophysiology* 45, no. 2: 198–210. https://doi.org/10.1016/0013-4694(78)90004-4.

Ponton, C., J. J. Eggermont, D. Khosla, B. Kwong, and M. Don. 2002. "Maturation of Human Central Auditory System Activity: Separating Auditory Evoked Potentials by Dipole Source Modeling." *Clinical Neurophysiology* 113, no. 3: 407–420. https://doi.org/10.1016/s1388-2457(01)00733-7.

Ponton, C. W., J. J. Eggermont, B. Kwong, and M. Don. 2000. "Maturation of Human Central Auditory System Activity: Evidence From Multi-Channel Evoked Potentials." *Clinical Neurophysiology* 111, no. 2: 220–236. https://doi.org/10.1016/s1388-2457(99)00236-9.

Poole, W., D. L. Gibbs, I. Shmulevich, B. Bernard, and T. A. Knijnenburg. 2016. "Combining Dependent *p* Values With an Empirical Adaptation of Brown's Method." *Bioinformatics* 32, no. 17: i430–i436. https://doi.org/10.1093/bioinformatics/btw438.

Pratt, H., A. Starr, H. J. Michalewski, N. Bleich, and N. Mittelman. 2008. "The Auditory P50 Component to Onset and Offset of Sound." *Clinical Neurophysiology* 119, no. 2: 376–387. https://doi.org/10.1016/j.clinph.2007.10.016.

Raul, P., E. Rowe, and J. J. A. Van Boxtel. 2024. "High Neural Noise in Autism: A Hypothesis Currently at the Nexus of Explanatory Power." *Heliyon* 10, no. 23: e40842. https://doi.org/10.1016/j.heliyon.2024.e40842.

Roberts, T. P., S. Y. Khan, M. Rey, et al. 2010. "MEG Detection of Delayed Auditory Evoked Responses in Autism Spectrum Disorders: Towards an Imaging Biomarker for Autism." *Autism Research* 3, no. 1: 8–18. https://doi.org/10.1002/aur.111.

Roberts, T. P., M. R. Lanza, J. Dell, et al. 2013. "Maturational Differences in Thalamocortical White Matter Microstructure and Auditory Evoked Response Latencies in Autism Spectrum Disorders." *Brain Research* 1537: 79–85. https://doi.org/10.1016/j.brainres.2013.09.011.

Roberts, T. P. L., L. Bloy, M. Ku, et al. 2020. "A Multimodal Study of the Contributions of Conduction Velocity to the Auditory Evoked Neuromagnetic Response: Anomalies in Autism Spectrum Disorder." *Autism Research* 13, no. 10: 1730–1745. https://doi.org/10.1002/aur.2369.

Roberts, T. P. L., E. S. Kuschner, and J. C. Edgar. 2021. "Biomarkers for Autism Spectrum Disorder: Opportunities for Magnetoencephalography (MEG)." *Journal of Neurodevelopmental Disorders* 13, no. 1: 34. https://doi.org/10.1186/s11689-021-09385-y.

Roberts, T. P. L., J. Matsuzaki, L. Blaskey, et al. 2019. "Delayed M50/M100 Evoked Response Component Latency in Minimally Verbal/Nonverbal Children Who Have Autism Spectrum Disorder." *Molecular Autism* 10, no. 1: 34. https://doi.org/10.1186/s13229-019-0283-3.

Ruiz-Martínez, F. J., E. I. Rodríguez-Martínez, C. E. Wilson, S. Yau, D. Saldaña, and C. M. Gómez. 2020. "Impaired P1 Habituation and Mismatch Negativity in Children With Autism Spectrum Disorder." *Journal of Autism and Developmental Disorders* 50, no. 2: 603–616. https://doi.org/10.1007/s10803-019-04299-0.

Sano, M., T. Hirosawa, Y. Yoshimura, et al. 2024. "Neural Responses to Syllable-Induced P1m and Social Impairment in Children With Autism Spectrum Disorder and Typically Developing Peers." *PLoS One* 19, no. 3: e0298020. https://doi.org/10.1371/journal.pone.0298020.

Sharma, A., J. Campbell, and G. Cardon. 2015. "Developmental and Cross-Modal Plasticity in Deafness: Evidence From the P1 and N1 Event Related Potentials in Cochlear Implanted Children." *International Journal of Psychophysiology* 95, no. 2: 135–144. https://doi.org/10.1016/j.ijpsycho.2014.04.007.

Sharma, A., N. Kraus, T. J. McGee, and T. G. Nicol. 1997. "Developmental Changes in P1 and N1 Central Auditory Responses Elicited by Consonant-Vowel Syllables." *Electroencephalography and Clinical Neurophysiology/Evoked Potentials Section* 104, no. 6: 540–545. https://doi.org/10.1016/s0168-5597(97)00050-6.

Sinclair, D., B. Oranje, K. Razak, S. Siegel, and S. Schmid. 2017. "Sensory Processing in Autism Spectrum Disorders and Fragile X Syndrome—From the Clinic to Animal Models." *Neuroscience & Biobehavioral Reviews* 76: 235–253. https://doi.org/10.1016/j.neubiorev.2016.05.029.

Stroganova, T. A., K. S. Komarov, O. V. Sysoeva, et al. 2020. "Left Hemispheric Deficit in the Sustained Neuromagnetic Response to Periodic Click Trains in Children With ASD." *Molecular Autism* 11, no. 1: 100. https://doi.org/10.1186/s13229-020-00408-4.

Stroganova, T. A., V. V. Kozunov, I. N. Posikera, I. A. Galuta, V. V. Gratchev, and E. V. Orekhova. 2013. "Abnormal Pre-Attentive Arousal in Young Children With Autism Spectrum Disorder Contributes to Their Atypical Auditory Behavior: An ERP Study." *PLoS One* 8, no. 7: e69100. https://doi.org/10.1371/journal.pone.0069100.

Sysoeva, O. V., K. Smirnov, and T. A. Stroganova. 2020. "Sensory Evoked Potentials in Patients With Rett Syndrome Through the Lens of Animal Studies: Systematic Review." *Clinical Neurophysiology* 131, no. 1: 213–224. https://doi.org/10.1016/j.clinph.2019.11.003.

Tian, B., D. Reser, A. Durham, A. Kustov, and J. P. Rauschecker. 2001. "Functional Specialization in Rhesus Monkey Auditory Cortex." *Science* 292, no. 5515: 290–293. https://doi.org/10.1126/science.1058911.

Uppenkamp, S., I. S. Johnsrude, D. Norris, W. Marslen-Wilson, and R. D. Patterson. 2006. "Locating the Initial Stages of Speech–Sound Processing in Human Temporal Cortex." *NeuroImage* 31, no. 3: 1284–1296. https://doi.org/10.1016/j.neuroimage.2006.01.004.

Walker, K. M., J. K. Bizley, A. J. King, and J. W. Schnupp. 2011. "Cortical Encoding of Pitch: Recent Results and Open Questions." *Hearing Research* 271, no. 1–2: 74–87. https://doi.org/10.1016/j.heares.2010.04.015.

Wang, X. 2007. "Neural Coding Strategies in Auditory Cortex." *Hearing Research* 229, no. 1–2: 81–93. https://doi.org/10.1016/j.heares.2007.01.019.

Wang, X. 2018. "Cortical Coding of Auditory Features." *Annual Review of Neuroscience* 41, no. 1: 527–552. https://doi.org/10.1146/annurev-neuro-072116-031302.

Wang, X., T. Lu, D. Bendor, and E. Bartlett. 2008. "Neural Coding of Temporal Information in Auditory Thalamus and Cortex." *Neuroscience* 154, no. 1: 294–303. https://doi.org/10.1016/j.neuroscience.2008.03.065.

Williams, Z. J., P. G. Abdelmessih, A. P. Key, and T. G. Woynaroski. 2020. "Cortical Auditory Processing of Simple Stimuli Is Altered in Autism: A Meta-Analysis of Auditory Evoked Responses." *Biological Psychiatry: Cognitive Neuroscience and Neuroimaging* 6, no. 8: 767–781. https://doi.org/10.1016/j.bpsc.2020.09.011.

Yoshimura, Y., T. Ikeda, C. Hasegawa, et al. 2021. "Shorter P1m Response in Children With Autism Spectrum Disorder Without Intellectual Disabilities." *International Journal of Molecular Sciences* 22, no. 5: 2611. https://doi.org/10.3390/ijms22052611.

Yoshimura, Y., M. Kikuchi, H. Hiraishi, et al. 2016a. "Synchrony of Auditory Brain Responses Predicts Behavioral Ability to Keep Still in Children With Autism Spectrum Disorder." *NeuroImage Clinical* 12: 300–305. https://doi.org/10.1016/j.nicl.2016.07.009.

Yoshimura, Y., M. Kikuchi, H. Hiraishi, et al. 2016b. "Atypical Development of the Central Auditory System in Young Children With Autism Spectrum Disorder." *Autism Research* 9, no. 11: 1216–1226. https://doi.org/10.1002/aur.1604.

Yoshimura, Y., M. Kikuchi, K. Shitamichi, et al. 2012. "Language Performance and Auditory Evoked Fields in 2- to 5-Year-Old Children." *European Journal of Neuroscience* 35, no. 4: 644–650. https://doi.org/10.1111/j.1460-9568.2012.07998.x.

Yoshimura, Y., M. Kikuchi, K. Shitamichi, et al. 2013. "Atypical Brain Lateralisation in the Auditory Cortex and Language Performance in 3- to 7-Year-Old Children With High-Functioning Autism Spectrum Disorder: A Child-Customised Magnetoencephalography (MEG) Study." *Molecular Autism* 4, no. 1: 38. https://doi.org/10.1186/2040-2392-4-38.

Yoshimura, Y., M. Kikuchi, S. Ueno, et al. 2014. "A Longitudinal Study of Auditory Evoked Field and Language Development in Young Children." *NeuroImage* 101: 440–447. https://doi.org/10.1016/j.neuroimage.2014.07.034.

Yoshimura, Y., Y. Mitani, T. Ikeda, et al. 2024. "Language and Sensory Characteristics are Reflected in Voice-Evoked Responses in Low Birth Weight Children." *Pediatric Research* 97, no. 1: 120–127. https://doi.org/10.1038/s41390-024-03270-9.

Supporting Information

Additional supporting information can be found online in the Supporting Information section. **Table S1:**—Absence of a significant main effect of group on P100m peak MNI coordinates: results of a mixed ANOVA. **Table S2:**. Time to half-maximum amplitude of the signal RMS for the auditory stimuli used in the experiment. **Figure S1:** Comparison of P100m maximum source positions in children scanned at 3T vs. 1.5T. **Figure S2:** Correlation Between P100m amplitude and MPI IQ in children with ASD and in typically developing children.